1972

Diffusiophoretic forces between juxtaposed atmospheric particles

Allen L. Williams

Department: Physics

DIFFUSIOPHORETIC FORCES BETWEEN JUXTAPOSED ATMOSPHERIC PARTICLES

by

ALLEN LEE WILLIAMS, 1947-

A DISSERTATION

Presented to the Faculty of the Graduate School of the

UNIVERSITY OF MISSOURI - ROLLA

In Partial Fulfillment of the Requirements for the Degree

DOCTOR OF PHILOSOPHY

in

PHYSICS

1972

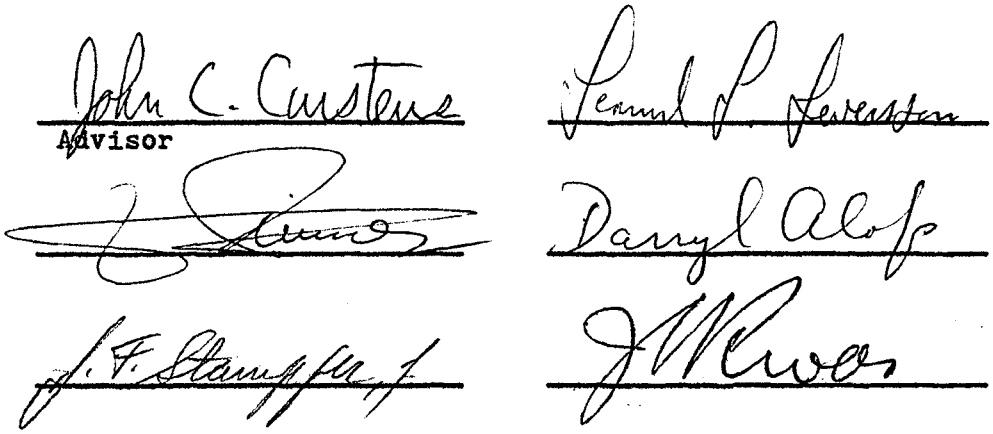

ABSTRACT OF THESIS

The role of diffusiophoretics and Stefan flow in droplet growth by accretion and in-cloud scavenging is examined. A calculation is made for the diffusive forces between two juxtaposed spheres one or both of which are undergoing diffusional growth and the influence of the diffusive force on the trajectories of two spheres, assumed to obey the creeping flow equations is found. The results are: a) the diffusiophoretic force between two water droplets is zero. b) the diffusiophoretic force between a spherical ice particle and a water droplet, although non-zero, is too small to appreciably influence the fall trajectories. c) the diffusiophoretic force between a growing, spherical cloud element and a spherical inert particle is large enough to enhance the collision efficiencies of the spheres.

ACKNOWLEDGEMENTS

The author wishes to thank Dr. J. C. Carstens for his advice and encouragement throughout the course of this study. Thanks are also due Dr. J. L. Kassner, Jr., Director of the Graduate Center for Cloud Physics Research, the staff, and graduate students of the Center for their many helpful suggestions. The author also wishes to thank Kathryn Berkbigler for her assistance in computer programming.

This research was supported by the Atmospheric Sciences Section, Office of Naval Research, under THEMIS Grant N00014-68-A-0497.

TABLE OF CONTENTS

LIST OF FIGURES

Figures Page

LIST OF TABLES

I INTRODUCTION

The present study concerns micro-physical processes occuring near cloud elements that are several microns in radius. Such a cloud element, say a growing droplet, serves as a sink of water vapor causing vapor to diffuse toward the surface. Another aerosol particle placed near the growing droplet may experience a momentum transfer due to the vapor flow toward the droplet, the result being a force on the aerosol particle. Although the calculation of this diffusive force is the main concern in this study, other related transport phenomena such as heat transfer due to the heat released by vapor condensation and the momentum transfer problem resulting from the gravitational settling of the particles will be considered as well.

One incentive for pursuing such an undertaking is to understand the processes leading to coagulation of atmospheric aerosols. The study of the coagulation processes is commonly divided into the study of the motion leading to collision and the determination of the chances of coagulation after collision. Situations contemplated usually involve only two bodies. The present study will be confined to the motion of particles without consideration of the actual collision process.

The results of calculations to determine the trajectories of two spheres moving in a viscous fluid under the assumptions of steady, creeping motion have shown that the spheres have a very slight chance of colliding. According to an analysis by Davis[1] of the resistance on each of two spheres approaching each other along the line joining

centers, the resistance increases from the Stokes value for an isolated sphere at separation between surfaces of about 10 radii to a value of about 60 times the Stokes resistance at a separation of .01 radii. For this reason two spheres that are on an apparent collision course may approach to a very small separation between surfaces, then "slide" around each other without colliding.

Of a particular concern in cloud physics is the development of non-freezing clouds. Under typical cloud conditions a droplet, once activated, can readily grow by diffusion to several microns radius, after which the radial growth becomes very slow. The above hydrodynamic considerations suggest that the growth of droplets by accretion is very sluggish for these small droplets. It is therefore not apparent how the cloud droplet size spectrum develops from droplets with radii of a few microns to sizes large enough to grow effectively by accretion.

Another atmospheric process that appears to be retarded by the nature of the hydrodynamic forces between two falling spheres (at least in the size range from a few microns radius to around 25 microns radius) is the scavenging of atmospheric particulates by cloud elements, called rainout for in-cloud scavenging and washout for below-cloud scavenging. Since the viscosity of water is much greater than that of air, the fluid streamlines near a water droplet are the same as those around a solid sphere of the same radius. (For droplets of the sizes considered, there is no appreciable internal circulation). The above hydrodynamic considerations, then, suggest that the collisions between either droplets or (spherical)

ice particles and (spherical) atmospheric particles are highly improbable.

Since the spheres can approach to very close separations without colliding, any mechanism that alters the trajectories only slightly for small separations could greatly enhance the possibility of collision. This fact has led to identification of a few of these mechanisms. For larger spheres (approximately 25 microns in radius) their inertia causes them to cross the creeping flow stream lines thus, in some cases, effecting collision. Although the particle inertia changes the flow trajectory only slightly, the effect is most pronounced for small sphere separations. Another phenomenon that can enhance the number of collisions is electrical forces between particles. Again, the force attains its largest value for small sphere separations, although for multi-pole interactions there may be angular dependence as well.

If one or both of the spheres is a cloud element undergoing diffusional growth or evaporation, diffusive forces may influence the trajectories. Diffusive forces resulting from a gradient of concentration of at least one component in a multi-component gaseous system can be discussed in terms of Stefan flow and diffusiophoresis. Consider two parallal plates maintained at equal temperatures and separated by a humid air mixture. Let one of the plates serve as a source of water vapor and the other a sink, both being of equal strength. After steady-state is attained there will exist a non-zero average molecular velocity of the vapor toward the condensing plate, while the average molecular velocity of the air will be zero.

From the non-vanishing average molecular velocity of the vapor one can calculate a total mass velocity representing a flow of the medium toward the condensing surface. The average mass velocity of the medium is called the Stefan velocity named after its discoverer J. Stefan.[2]

Diffusive forces can also exist in the absence of a source or sink. Let the plates be replaced by vessels of equal temperature and pressure, each containing a different gas and connected by a tube of small diameter compared to the size of the vessels. If this system is allowed to attain steady-state, the total pressure in the tube will be constant and there will exist equal and opposite concentration gradients of the two gases. If the molecular weights of the two gases are not equal there will be a mass flow in the direction of the heavier gas component. A small particle placed in this tube would experience a force due to the gas flow around it. The term diffusiophoresis will be used to designate both this phenomenon and the similar situation resulting from Stefan flow.

The diffusiophoretic force on a particle depends on the value of the vapor density gradient established in the neighborhood of the particle. For an isolated growing cloud element the density gradient has its largest magnitude at the surface and falls off radially. If a particle is placed near the cloud element, it should experience a diffusive force due to the flow of water vapor toward the growing cloud element, the force being larger for smaller separations. (Neglected here is the possibility that the presence of the particle may change the vapor density profile.) To the extent that the

diffusive forces oppose the hydrodynamic forces caused by gravitational settling, the fall trajectories of the particles will be influenced in favor of collision.

The present effort is directed toward determining the extent to which diffusiophoretic forces affect the two-sphere trajectories from the standpoint of continuum hydrodynamics. An attempt will be made to keep the analysis general in the sense that a juxtaposition of two particles both undergoing diffusional growth or evaporation (denoted as volatile particles) will be considered, as well as the situation in which one of the particles is volatile the other inert (not undergoing diffusional growth or evaporation). The parameters that identify the particles such as the thermal conductivities and latent heats, will be kept distinct so that, for example, if both spheres are volatile one may correspond to a water droplet, the other an ice particle.

II REVIEW OF LITERATURE

The calculations of diffusiophoretic forces differ depending upon the particular Kundsen number regime considered.[3] The Kundsen number is defined as $K = \lambda/R$ where R is the radius of the sphere suspended in a fluid of mean-free path λ. In the regime of large Kundsen number, the free-molecule regime, where $K \to \infty$ the transport processes occuring in the system can be described using uniform kinetic theory. This type of analysis can be extended to the transition regime ($10 > K_n > 10^{-1}$) by using the kinetic theory of non-uniform gases. In this regime, the distribution of molecules in the medium is influenced by the presence of the particle surface. This problem is further complicated by the lack of a reliable theory for the distribution of molecules leaving the surface.

In the continuum regime, defined in the limit as K_n approaches zero, the transport phenomena in the fluid can be described by the laws of continuum mechanics. It has been found by comparison with experiment that the continuum approach can be extended to the so called slip flow regime ($10^{-1} > K_n > 10^{-2}$) by using velocity slip and temperature jump boundary conditions.

If there exists a density gradient of one component of a binary mixture tangent to any surface in the system, the possibility of diffusion slip along this surface must be considered. Diffusion slip was first investigated by Kramers and Kistemaker[4](1943). They measured the slip velocity tangent to a wall along which was established a density gradient. Using a kinetic theory calculation, they found an expression for the diffusion slip coefficient. In the

usual continuum analysis of a gas flowing tangential to a stationery surface, the gas velocity evaluated at the surface is taken to be zero. However, the velocity of a gas diffusing along a surface is not always taken as zero. Diffusion slip represents a compromise in that, if a density gradient exists tangential to a surface, the velocity of the gas at the surface will take on some value between zero and the Fick's Law velocity. This diffusion slip phenomena influences the way in which momentum is transferred to a particle present in a diffusing gas mixture and thus may be of importance for the description of the diffusiophoretic force on a particle in the slip-flow and continuum regimes.

A. DIFFUSIOPHORESIS

Early research into what is now called diffusiophoresis was reported by Aitken[5] (1883) whose results were later confirmed by Watson[6] (1936). They essentially observed a dust free zone near an evaporating surface. Facy[7,8,9] (1955) observed not only a dust free space near an evaporating droplet, but an increase in the number of dust particles near a condensing surface and a general movement of the particles toward the surface, with some being absorbed.

Deryagin and Dukhin[10] (1956) first calculated the force on an inert particle in a constant density gradient. They considered the velocity field of the medium to be the Stefan velocity which, in this case, is the average mass velocity of the gaseous medium. They found the velocity of the particle to be the same as the Stefan velocity far removed from the particle. Deryagin and Dukhin[11] also calculated the force on a volatile particle in a diffusing gas mixture. In this case they found that in addition to the Stefan flow force, there is another force arising from the density gradients near the particle, causing a force opposing the Stefan flow. They concluded that, if the external concentration gradient is set up by a phase change of the same material as the droplet, the total force on the droplet is zero. (This result was later contradicted in a calculation by Deryagin and Yalamov.[20]) The force on a volatile particle in both an externally imposed temperature and density gradient was found by Dukhin and Deryagin.[12] The velocity field of the gas medium was found by solving the Navier-Stokes equation for

creeping, steady motion, the equation of continuity for incompressable flow, and the steady-state, non-convective forms of Fick's law of diffusion, and Fouriers law of heat conduction simultaneously, subjected to the usual continuum boundary conditions (neglecting diffusion slip). According to this analysis the force on two widely separated water droplets is zero.

Waldmann (1961)[13] found expressions for the forces on an inert particle in a diffusing gas mixture. Diffusion slip was accounted for in this analysis. The force on a particle in a binery gas mixture, each component of which is diffusing in opposite directions, was found to be in the direction of the heavier gas component. He also examined the situation of an inert particle suspended in a carrier gas through which vapor is diffusing. Although these results gave the proper direction for the forces, they do not agree with the experimental results of Schmitt and Waldmann[14,15] and of Schmitt.[16] Waldmann, therefore, proposed an empirical expression for the diffusion slip factor which led to reasonable experimental agreement.

Brock[17] (1963) derived a new expression for the diffusion slip coefficient and using it calculated the force on an inert sphere suspended in a diffusing gas mixture. This analysis gave results very similar to those presented by Waldmann and can be shown to give identical results if the diffusion slip coefficients are set equal. Brock's slip coefficient depends on the accommodation coefficients of each species to the particle surface. Since there is no experimental information available on the accommodation coefficients of each chemical species in a mixture, the question of

diffusion slip is still open.

A completely different approach to the problem of diffusiophoresis has been taken by Deryagin et. al.[18,19,20] (1966). In this approach they considered two vessels containing binary gas mixtures, between which is maintained concentration and pressure differences. The vessels are separated by an "aerosol partition". Using irreversible thermodynamic arguments, they calculated the force on the aerosol particles in the partition. Diffusion slip was regarded as only of minor importance and was neglected in this development. The force calculated in this way gave reasonable agreement with the experimental value of the repulsive diffusiophoretic force between a silver coated glass sphere and an evaporating droplet as reported by Prokhorov and Leonov.[21]

There are thus two general approaches to the problem of calculating diffusiophoretic forces. The approach taken by Waldmann and Brock, as well as the earlier attempts by Deryagin's group, are based on hydrodynamic considerations, the basic differences being related to the question of diffusion slip. The non-equilibrium thermodynamic approach appears to be quite different in the method of attack. Unfortunately there is a scarcity of experimental data to determine which of the theories for calculation of the diffusiophoretic force on large particles is correct. Even the question of the effect of diffusion slip on the particle motion has not been satisfactorily resolved. With regard to the irreversible thermodynamic approach, Waldmann[22] has raised some questions regarding certain boundary conditions used.

For the problem at hand the conventional hydrodynamic approach will be exploited, admitting, however, that the irreversible thermodynamic approach may lead to equally suitable results. The existance of diffusion slip will be acknowledged and used in the subsequent development. By setting the slip coefficient equal to zero, the condition of no slip at the particle surface can be realized.

Corresponding to the diffusiophoretic forces which occur due to density gradients in the system, there exist thermophoretic forces which result from thermal gradients in the system. Due to the similarities of these two phenomena, thermophoresis has been developed by essentially the same researchers as diffusiophoresis. For the systems considered in this work, the thermophoretic forces are much smaller [23,24] than the diffusiophoretic forces and will therefore be neglected in the present work.

There has been very little experimental work done to determine the continuum motion of particles in a diffusion field. Prokhorov and Leonov[21] have presented results for the long-range diffusion forces between water droplets and non-volatile particles. They were, however, troubled by convection currents due to the cooling of the droplet from evaporation. To avoid the convection problem they had to heat the droplet to the same temperature as the surrounding medium. There has been no work reported for the diffusion forces on closely spaced spheres in the continuum regime.

Some work has been done to determine the atmospheric significance of diffusiophoresis for small particles. Goldsmith et. al.[25] found an experimental expression for the velocity of deposition of

small particles (about 1 micron radius) on a sulfuric acid surface. Based on this velocity, Goldsmith and May [26] presented a calculation to determine the role of diffusiophoresis in the scavenging of these particles from the atmosphere by growing water drops. They concluded that diffusiophoresis plays a very minor role in atmospheric scavenging. In this calculation they did not consider the drops to be falling due to gravity. Since a falling drop comes into proximity with more particles than a stationery drop and the diffusiophoretic force is larger for close separations, it is not clear that gravitational fall and the subsequent hydrodynamic problem can be ignored. Also neglected here is the heat liberated at the droplet durface due to condensation.

Using an analogy between the vapor density profile about a growing drop and the electric potential around a conducting sphere, Podzimek[27] investigated the binding of small AgI particles onto growing droplets and ice crystals. The distribution of vapor around the droplets and ice crystals was found by measuring the electrostatic field in an electrolytical vessel. The velocity of the particles was then calculated by using the Goldsmith velocity expression. The results indicate that the scavenging of small atmospheric particles may be important in mixed clouds. Again the results were not interpreted for a falling droplet or ice crystal.

According to the laboratory work of Vittori and Prodi[28], ice particles are 16 times more efficient than water droplets in scavenging small atmospheric particles. They also reported[29] that the observed velocity of particles in a density gradient is slower than

the Stefan flow.

Field experiments to examine the concentrations of different sized solid, water-insoluble particles in rainwater and hailstones were reported by Rosinski.[30] He concluded that "Stefan flow is probably the predominant mechanism of in-cloud scavenging of particles 1.5 - 5 microns in diameter when solid (ice crystal) and liquid (supercooled droplet) phases are present simultaneously."

B. HYDRODYNAMIC RESULTS

As a result of several contributions, the hydrodynamic problem of the steady, creeping motion of two spheres settling in a viscous fluid has been solved for different sized spheres and for arbitrary orientation. The assumptions of steady, creeping motion will be examined in the next section. The general motion of the spheres has been divided into motion parallel to the line of centers and motion perpendicular to the line of centers. Some remarks on this division of the velocity field will also be presented later.

An attempt to determine the motion of two spherical atmospheric particles moving in a viscous fluid under the assumptions of steady, creeping flow and in the absence of diffusion was reported by Hocking in his Ph.D. thesis[31] (1958). Hocking's method of solution involved solving a large (in the limit infinite) set of simultaneous equations. The approximate solution was found by solving the first several members of the set of equations. The often quoted result of Hocking's work is that spheres with radii less than 19 microns do not collide.

An exact expression for the steady, creeping motion of two spheres moving with equal velocities parallel to their line of centers was derived by Stimpson and Jeffery[32] (1926). Maude[33] (1961) and Brenner[34] (1961) independently extended the Stimpson and Jeffery solution to include the motion of two spheres moving with arbitrary velocities along their line of centers. Using this solution along with the solution used by Hocking for motion perpendicular to the line of centers (probably due to Wakiya[35]), Davis and Sartor[36] (1967)

calculated collision efficiencies which were quite different from Hocking's original deduction. The new calculation failed to show the 19 micron cut-off. However, collision efficiencies for spheres of less than 20 microns in radius were still found to be quite small.

The mathematical analysis for a sphere moving parallel to a rigid infinite plane in steady, creeping flow was presented by O'Neill[37] (1964) based on a previous calculation by Dean and O'Neill[38] in 1963. The problem was done in bispherical coordinates enabling Wakiya[39] (1967) to generalize the problem to include two equal or unequal spheres moving perpendicular to their line of centers. Some numerical results for this motion were presented by Davis[40] (1969) who used the solution given by Wakiya.

A whole chapter in the book by Happel and Brenner[41] (1965) is devoted to the discussion of the two sphere hydrodynamic problem. Calculations for the motion of two arbitrarily oriented equal spheres, as well as comparison with experimental results is given by Goldman, Cox, and Brenner[42] (1966). The agreement with the experimental results of Eveson, Hall, and Ward[43] (1959) for which the Reynolds number never exceeded .018 is very good, to within 5 percent for values of a/h ranging from .097 to 1.0 where a is the sphere radius and h one-half the distance between centers. Theory and experiment both reveal that the small amount of rotation that does occur affects the sphere trajectories very slightly.

Other experiments on the settling of two equal, arbitrarily oriented spheres were done by Mathews and Smith[44], Slack and Mathews,[45] and by Jayaweera, Mason, and Slack.[46] These investigators observed

the upper sphere to overtake the lower sphere which does not agree with theoretical predicitions for viscous flow around, equal spheres. The discrepancy is apparently inertial in origin. This is borne out by Klett[47] in his thesis where the Oseen correction is applied to two-sphere motion. Klett concludes that the inertial effects are important even for Reynolds numbers as low as .03 which corresponds to water droplets in air of radius 15 microns. Care must be taken when extending these experimental results, which were taken for solid spheres settling in a liquid medium, to atmospheric situations where the medium is gaseous.

III THEORY

The gas-particle system considered here will consist of spherical cloud elements of approximately 10 microns in radius suspended in a humid air environment. Since the molecular mean free path of the gas is about 6×10^{-6} cm., the Knudsen number is much smaller than unity. In view of this, the transport properties of the system can be described by the laws of continuum mechanics. Except for diffusion slip, the usual continuum boundary conditions will be employed. Although diffusion slip will be included, the complete continuum approach can be realized by setting the slip coefficient equal to zero. Due to the uncertainty regarding the continuum analysis of the fluid flow between two closely separated spheres, separations of less than about one micron will not be considered.

In order to find the force on particles suspended in a fluid, the mass velocity, $\bar{v}$, and the pressure, P, in the fluid must be established. The stress tensor can then be calculated from these fields. By integrating the stress tensor over the surface of the particles in the fluid, the force on the particles can be found.

Consider two spherical particles, one or both of which are volatile, suspended in an incompressible fluid, the whole system being in a constant gravitational field. The equation of motion of the fluid is:

$$\rho \frac{\partial \bar{v}}{\partial t} + \rho(\bar{v} \cdot \bar{\nabla})\bar{v} = -\bar{\nabla}P + \eta\nabla^2 \bar{v} + \rho\bar{g} \quad , \tag{1}$$

where ρ is the total mass density of the fluid, η the fluid viscosity, $\bar{g}$ the acceleration of gravity and t the time. The

equation of continuity for incompressible flow implies

$$\bar{\nabla} \cdot \bar{v} = 0. \tag{2}$$

The equation for heat transfer can be written[48]

$$\frac{\partial T}{\partial t} + (\bar{v} \cdot \bar{\nabla}) T = \chi \nabla^2 T. \tag{3}$$

Here T is the temperature at any point in the system and $\chi = K/(\rho C_p)$, where K is the thermal conductivity at the position considered with mass density ρ and specific heat at constant pressure C_p. Diffusion of the water vapor of mass density ρ_v can be described by the equation:[49]

$$\frac{\partial \rho_v}{\partial t} + (\bar{v} \cdot \bar{\nabla}) \rho_v = D \nabla^2 \rho_v \tag{4}$$

where D is the diffusion coefficient. According to a perturbation analysis by Brock[17,50,51] the second term in both equations (3) and (4) can be neglected for the present system.

If one defines characteristic parameters such as the radius of one of the spheres, R(for closely spaced spheres the characteristic length may be best described as the distance between surfaces), and the free stream velocity, V, far away from both spheres, the Navier-Stokes equation can be expressed in terms of these quantities. The ratio of the inertial term to the viscous term then becomes $Re = \rho VR/\eta$, where Re is the Reynolds number. For an isolated sphere of 10 microns radius falling in air, the Reynolds number is of order 10^{-2}. Using this value for the present situation, the inertial term in the equation can be neglected in favor of the viscous term. Further justification for dropping the inertial term

appeals to the accuracy of such a calculation for falling, equal spheres when compared with experiment as discussed earlier.

Since the second term on the left of equation (3) can be neglected the heat equation becomes:

$$\frac{\partial T}{\partial t} = \chi \nabla^2 T.$$

A solution to this equation for a point source is given by Landeau and Lifshitz[48]. The characteristic time required for heat to be conducted to a distance ℓ from the source is $\tau \sim \ell^2/\chi$. This time can also be interpreted as the time necessary for the temperature of a non-uniformly heated body of dimension ℓ to become more or less constant throughout. Calling ℓ the distance between surfaces of two juxtaposed spheres, the temperature profile between the spheres reaches a steady value in a time $\tau = \ell^2/\chi \sim 10^{-4}$ sec for $\ell = 50$ microns. During this time the spheres will settle to a new position resulting in a slight change in the temperature profile. This change in the profile with respect to time is very small compared to the changes contemplated for the whole trajectory. Therefore, the usual steady-state approximation will be made yielding for the heat conduction equation:

$$\nabla^2 T = 0. \qquad (3')$$

The diffusion equation has exactly the same form and the above analysis applies to it as well. The mass diffusion equation therefore reduces to:

$$\nabla^2 \rho_v = 0. \qquad (4')$$

Taking the curl of each term in the Navier-Stokes equation

(equation 1) and defining the vorticity as:

$\Omega = \bar{\nabla} \times \bar{v}$, equation 1 reduces to:

$\frac{\partial \Omega}{\partial t} = \eta/\rho \nabla^2 \Omega$. This has the same form as the heat conduction equation, so the relaxation time needed for the vorticity to reach its steady-state value is $\tau \sim \ell^2 \rho / \eta$. For a given value of ℓ this relaxation time is of the same order of magnitude as for heat conduction and diffusion, so the same argument for the steady-state approximation can be used. (Note that as the sphere separation is decreased the approximation becomes stronger.) A particle moving in steady flow is necessarily moving in such a way as to make the total force on the particle zero. Thus for the situation considered here, the gravitational force on the particle and the hydrodynamic forces must sum to zero.

Since the density of the particles is much greater than that of their environment the buoyancy force on the particles, represented by the last term in (1), can be neglected. The equation of motion of the fluid therefore reduces to:

$$\overline{\nabla p} = \eta \nabla^2 \bar{v}. \qquad (1')$$

As pointed out by Berker[52] and Brenner,[53] since these equations of motion and the boundary conditions (to be discussed later) are linear functions of velocity and pressure, the problem of the general motion of two spheres satisfying equations (1') and (2) can be decomposed into a number of simpler problems. For example, the velocity can be written as the sum of other velocities say $\bar{v} = \bar{v}_1 + \bar{v}_2$ and the pressures corresponding to each of these velocities become $P = P_1 + P_2$. If these parameters satisfy the

equations

$$\overline{\nabla P_1} = \eta \nabla^2 \bar{v}_1 \quad , \quad \overline{\nabla P_2} = \eta \nabla^2 \bar{v}_2 \, ,$$

$\nabla \cdot \bar{v}_1 = 0$, and $\nabla \cdot \bar{v}_2 = 0$ subject to boundary conditions consistent with the boundary conditions of the total flow field, then solving each of the sub-problems is equivalent to solving the original problem. Brenner also shows that a stress tensor and hence a force, can be found from each of the individual flow fields, the total force being a sum of each of the smaller forces. For the problem at hand, it is convenient to separate the hydrodynamic problem into three parts. These are motion perpendicular and parallel to the line of centers due to gravitational settling, and motion due to diffusiophoretic forces. The problem of gravitational settling has been solved, as discussed in the literature review. Once the diffusiophoretic force is known, the velocity of each particle for any separation can be found by requiring that the total force on the particles be zero.

Consider then two juxtaposed particles, at least one of which is growing by diffusion, positioned in an otherwise quiescent fluid. From the axisymmetric geometry of this configuration, any force present must be along the line of centers of the spheres. The spheres will be constrained not to move and the necessary force of constraint will be found by solving equations (1') and (2) for the velocity and pressure fields due to diffusion. At the surface of a volatile particle the boundary conditions on the velocity are:

$$\bar{v} \cdot \bar{n} \Big|_{\text{SURFACE}} = \frac{-D}{\rho_g} \left(\overline{\nabla \rho_v} \cdot \bar{n} \right) \Big|_{\text{SURFACE}} \qquad (5)$$

and

$$\bar{v} \cdot \bar{\tau} \Big|_{SURFACE} = - \frac{\sigma D}{\rho_g} \left(\overline{\nabla \rho_v} \cdot \bar{\tau} \right) \Big|_{SURFACE} . \qquad (6)$$

Here $\bar{n}$ and $\bar{\tau}$ are unit vectors normal and tangential to the particle surface respectively, ρ_v the mass density of the water vapor, D the diffusion coefficient of the binary gas system, ρ_g the density of the dry air, and σ the diffusion slip coefficient first derived by Kramers and Kistemaker.[4] For an inert particle no vapor can penetrate the surface. Writing the condition of impenetrability as

$$\overline{\nabla \rho_v} \cdot \bar{n} \Big|_{SURFACE} = 0 \quad , \qquad (7)$$

it is apparent that the fluid velocity normal to the particle surface as described by equation (5) must be zero. The tangential velocity will have the same form as shown in equation (6). In fact, the velocity boundary conditions for both inert and volatile particles can be described by equations (5) and (6), the difference being that the density profile will be different in each case.

Neglecting temperature jump at the particle surface, the temperature at the surface of both inert and volatile particles must be continuous, that is:

$$T_e \Big|_{SURFACE} = T_i \Big|_{SURFACE} \quad , \qquad (8)$$

where T_e is the temperature external to the particle and T_i the internal temperature.

A droplet that is undergoing diffusional growth must conduct away any heat released at the surface either via the outside medium or into the droplet. This can be expressed in terms of a steady-state power balance:

$$\bar{n} \cdot \{ LD \overline{\nabla \rho_v} + K_e \overline{\nabla T_e} - K_i \overline{\nabla T_i} \} \Big|_{SURFACE} = 0. \qquad (9)$$

Here L is the latent heat of the volatile particle, K_e the thermal conductivity external to the particle, and K_i that internal to it. If the particle is inert the condition of impenetrability reduces equation (9) to $\bar{n} \cdot \{ K_e \overline{\nabla T_e} - K_i \overline{\nabla T_i} \} = 0.$ (10)

It will be assumed that the temperature and vapor density are in equilibrium at the droplet surface. This assumption is good under the condition that $(\lambda / R\, \vartheta) >> 1$ (see Carstens and Kassner,[54] 1968) where ϑ is the sticking coefficient. (Actually these same criteria determine the validity of the thermal continuity boundary condition as well.) The condition of thermal equilibrium, therefore, becomes: $\rho_v \Big|_{SURFACE} = bT \Big|_{SURFACE} + c$ (11)

where b and c are constants determined from experiment.

Far from the particles, the temperature and vapor density must attain their bulk values so: $\rho = \rho_\infty$ and $T = T_\infty$ at an infinite distance from the spheres. Also at an infinite distance from the spheres, there can be no fluid motion caused by diffusion since there are no density gradients thus $\bar{v} = 0$ at infinity.

In the more general situation the differential equations describing the temperature, vapor density, velocity, and pressure fields are coupled such that all four equations must be solved simultaneously. In the system considered here, approximations have been made which decouple the pressure and velocity fields

from the temperature and density fields. In what follows, the temperature and density profiles will be found by simultaneously solving equations (3') and (4'). These solutions will be subjected to boundary conditions (7), (8), and (10) at the surface of an inert particle and boundary conditions (8), (9), and (11) if the particle is volatile. Once the vapor density profile for the system is known, the pressure and velocity fields can be found by simultaneously solving equations (1') and (2) subject to boundary conditions (5) and (6).

A. TEMPERATURE AND VAPOR DENSITY PROFILES

Due to the geometry of the system, a bispherical coordinate system will be used to find the profiles. A review of bispherical coordinates may be found in Happel and Brenner[41] or Morse and Feshbach.[55] Figure 1 shows the coordinate grid. The full three dimensional system is obtained by rotating this system about the z - axis.

The solutions to equations (3') and (4') in bispherical coordinates are:

$$T_e = T_\infty + \sqrt{f} \sum_{n=0}^{\infty} [A_n \exp(-\mu_n) + B_n \exp(\mu_n)] P_n(w) \quad \text{and} \tag{12}$$

$$\rho_v = \rho_\infty + \sqrt{f} \sum_{n=0}^{\infty} [C_n \exp(-\mu_n) + D_n \exp(\mu_n)] P_n(w) \quad \text{for } -\mu_2 \leq \mu \leq \mu_1 , \tag{13}$$

$$T_1' = \sqrt{f} \sum_{n=0}^{\infty} F_n' \exp(-\mu_n) P_n(w) \quad \text{for } \mu \geq \mu_1 , \tag{14}$$

$$T_1'' = \sqrt{f} \sum_{n=0}^{\infty} F_n'' \exp(\mu_n) P_n(w) \quad \text{for } \mu \leq -\mu_2 . \tag{15}$$

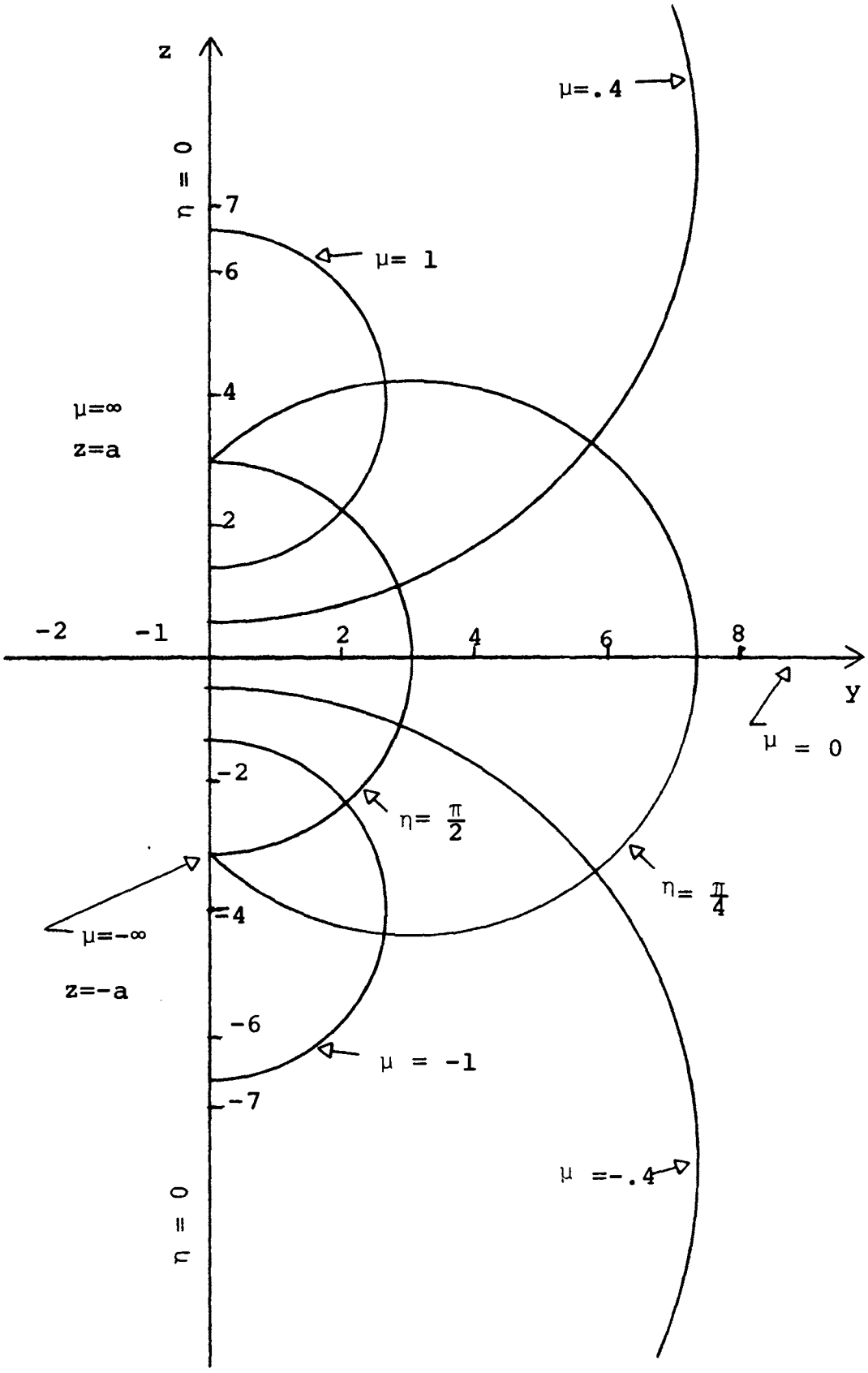

Figure 1. The Bispherical Coordinate System.

Here A_n, B_n, C_n, D_n, F_n' and F_n'' are arbitrary constants to be determined from the boundary conditions, ρ_∞ and T_∞ are the ambient values of temperature and vapor density, $\mu_n = (n+\frac{1}{2})$, $w = \cos\eta$, and $f = \cosh\mu - w$. μ_1 describes the surface of particle 1 with center on the positive z-axis and $-\mu_2$ describes the surface of particle 2 centered on the negative z-axis. (The minus sign associated with μ_2 will be carried along explicitly so μ_2 is a positive number.)

These equations have been solved and the profiles computed for two juxtaposed water droplets by Carstens, Williams, and Zung[56] (1970) with comments by Williams and Carstens[57] (1971). The calculations will be generalized here to include particles with distinct latent heats and thermal conductivities. Also, the profiles will be found for an inert and volatile particle juxtaposition.

For the situation in which both particles are volatile the boundary conditions yield:

$$A_n - F_n' + B_n \exp(2\mu_{n1}) = -\sqrt{2}\, T_\infty \tag{16}$$

and

$$A_n \exp(2\mu_{n2}) + B_n - F_n'' = -\sqrt{2}\, T_\infty \tag{17}$$

from thermal continuity at particles 1 and 2 respectively,

$$C_n - b_1 F_n' + D_n \exp(2\mu_{n1}) = \sqrt{2}(C_1 - \rho_\infty) \tag{18}$$

and

$$C_n \exp(2\mu_{n2}) + D_n - b_2 F_n'' = \sqrt{2}(C_2 - \rho_\infty) \tag{19}$$

from thermal equilibrium,

$$\alpha_n = n\alpha_{n-1}' + (n+1)\alpha_{n+1}' \tag{20}$$

and

$$\beta_n = n\beta'_{n-1} + (n+1)\beta'_{n+1} \tag{21}$$

from the power balance. The following notation has been used: $\mu_{n1} = (n+\frac{1}{2})\mu_1$, $\mu_{n2} = (n+\frac{1}{2})\mu_2$, b_1, b_2, c_1, c_2 are the constants obtained by requiring thermal equilibrium at each surface, K_{i1}, K_{i2}, K_e are the thermal conductivities of particle 1, particle 2, and the medium external to the particles, L_1 and L_2, are the latent heats of condensation (sublimation) of particles 1 and 2, D the diffusion coefficient,

$$\alpha_n = T_{11}(C_n + \Gamma_{e1}A_n - \Gamma_{i1}F'_n)\exp(-\mu_{n1}) + T_{12}(D_n + \Gamma_{e1}B_n)\exp(\mu_{n1}),$$

$$\alpha'_n = -(C_n + \Gamma_{e1}A_n - \Gamma_{i1}F'_n)\exp(-\mu_{n1}) + (D_n + \Gamma_{e1}B_n)\exp(\mu_{n1}),$$

$$\beta_n = T_{22}(C_n + \Gamma_{e2}A_n)\exp(\mu_{n2}) + T_{21}(D_n + \Gamma_{e2}B_n + \Gamma_{i2}F''_n)\exp(-\mu_{n2}),$$

$$\beta'_n = (C_n + \Gamma_{e2}A_n)\exp(\mu_{n2}) - (D_n + \Gamma_{e2}B_n + \Gamma_{i2}F''_n)\exp(-\mu_{n2}),$$

$$T_{11} = \sinh(\mu_1) - (2n+1)\cosh(\mu_1),$$

$$T_{12} = \sinh(\mu_1) + (2n+1)\cosh(\mu_1),$$

$$T_{21} = \sinh(\mu_2) - (2n+1)\cosh(\mu_2),$$

$$T_{22} = \sinh(\mu_2) + (2n+1)\cosh(\mu_2),$$

$$\Gamma_{e1} = \frac{K_e}{L_1 D}, \quad \Gamma_{e2} = \frac{K_e}{L_2 D}, \quad \Gamma_{i1} = \frac{K_{i1}}{L_1 D}, \quad \Gamma_{i2} = \frac{K_{i2}}{L_2 D}.$$

Each of equations (16-21) yield a separate equation for each value of n. Consider the case for n=0, equations (16-19) give four equations and six unknowns. Equations (20) and (21) add two more equations and six more unknowns, since for n=0, α'_{n+1} and β'_{n+1} give the n=1 order constants. It appears that two more conditions are needed to specify the solution. This situation can be alleviated by summing the power balance boundary condition over every point on the surface of each of the spheres. For particle 1 this condition can be written:

$$\iint \bar{n} \cdot \{\overline{\nabla \rho_v}\Big|_{\mu=\mu_1} + \Gamma_{e1} \overline{\nabla T_e}\Big|_{\mu=\mu_1} - \Gamma_{i1} \overline{\nabla T'_i}\Big|_{\mu=\mu_1}\} dS = 0$$

where $\bar{n}$ is a unit vector normal to the surface. This condition yields at surface 1 and 2 respectively:

$$\sum_{n=0}^{\infty} (D_n + \Gamma_{e1} B_n) = 0, \tag{22}$$

$$\sum_{n=0}^{\infty} (C_n + \Gamma_{e2} A_n) = 0. \tag{23}$$

Consider the situation in which one of the particles is inert and the other volatile. Enforcing the volatile boundary conditions at surface 1 yields equations (16), (18), (20) and (22). At the surface of the inert particle thermal continuity holds, thus equation

(17) is valid. The condition of impenetrability, equation (7), enforced at surface 2 gives:

$$\gamma_n = n\,\gamma'_{n-1} + (n+1)\,\gamma'_{n+1} \tag{24}$$

where $\gamma_n = T_{22}\,C_n \exp(\mu_{n2}) + T_{21}\,D_n \exp(-\mu_{n2})$

and $\gamma'_n = C_n \exp(\mu_{n2}) + D_n \exp(-\mu_{n2})$.

The power balance condition at surface 2 can again be written as equation (21), however, some simplifications can be made due to the condition of impenetrability. Integrating the power balance and the condition of impenetrability over surface 2 yields:

$$\sum_{n=0}^{\infty} A_n = 0 \quad \text{and} \quad \sum_{n=0}^{\infty} C_n = 0 \quad . \tag{25}$$

These boundary condition equations are sufficient to specify unique values of the arbitrary constants in equations (12) - (15) for juxtapositions of both two volatile particles and one inert particle the other volatile. Numerical values for the constants were found on an IBM - 360 computer. The approximate temperature and vapor density profiles were then found by taking a sufficient number of terms in the summation expressions for the temperature and vapor density. The constants either remained the same or converged for increasing values of n, making possible a solution accurate to several decimal places by taking less than ten terms in the sums.

B. DIFFUSIOPHORETIC FORCE

Before calculating the force, it will prove expedient to simplify the velocity boundary conditions. This can be done by noting that the force calculation can be reduced to a number of sub-problems as discussed earlier. Consider the velocity division $\bar{v} = \bar{v}' + \overline{\nabla \phi}$ where ϕ is any scalar function. The pressure gradient corresponding to the velocity $\overline{\nabla \phi}$ and the resulting force are zero,[13] so this amounts to a trivial division, It is then apparent that the gradient of any scalar function can be added to the velocity field without changing the force due to this velocity.

Consider the diffusional velocity field

$\bar{v} = \nabla \overline{\frac{D\rho_v}{\rho_g}} \sim \frac{D}{\rho_g} \overline{\nabla \rho_v}$, where terms of order $\overline{\nabla \rho_v} \cdot \overline{\nabla \rho_g} / \rho_g^2$ are neglected. This velocity can be added to the total diffusion velocity field changing the surface boundary conditions, equations (5) and (6), yielding:

$$\bar{v} \cdot \bar{n} \Big|_{SURFACE} = 0 \quad \text{and} \tag{26}$$

$$\bar{v} \cdot \bar{\tau} \Big|_{SURFACE} = (1 - \sigma) \frac{D}{\rho_g} \left(\overline{\nabla \rho_v} \cdot \bar{\tau} \right) \Big|_{SURFACE} . \tag{27}$$

Since the vapor density far from the particle surfaces is at its bulk value and, hence, constant the gradient velocity is zero. The condition on the velocity far from the surface, therefore, remains zero.

Since the diffusion flow field has axisymmetric geometry, a stream function representing the solution to equations (1') and (2) can be used. According to Stimpson and Jeffery[32] the stream

function in bispherical coordinates for this situation can be written as:

$$\Psi = f^{-3/2} \sum_{n=0}^{\infty} U_n V_n(w) \tag{28}$$

where $U_n = A_n' \cosh(n - \frac{1}{2})\mu + B_n' \sinh(n - \frac{1}{2})\mu$

$+ C_n' \cosh(n + \frac{3}{2})\mu + D_n' \sinh(n + \frac{3}{2})\mu$.

Here A_n' , B_n' , C_n' , and D_n' are constants to be determined and

$V_n(w) = C_{n+1}^{-\frac{1}{2}}(w)$ where C_n^{-m} are the Gegenbauer Polynomials defined by:

$$\sum_{n=0}^{\infty} C_n^m(x)\, t^n = (1 - 2xt + t^2)^{-m}$$

The velocities normal and tangential to the sphere surfaces as related to the stream function are:[41]

$$\bar{v} \cdot \bar{n} = \frac{f^2}{a^2} \frac{\partial \Psi}{\partial w} \quad \text{and} \tag{29}$$

$$\bar{v} \cdot \bar{\tau} = \frac{f^2}{a^2 \sin\eta} \frac{\partial \Psi}{\partial \mu} \quad . \tag{30}$$

Here a is a constant used in bispherical coordinates for a particular sphere separation defined as $a = (d^2 - r^2)^{\frac{1}{2}}$, where

d is the distance along the z-axis to the center of the sphere of radius r. The boundary condition for velocity normal to the surface in terms of the stream function becomes:

$$\left.\frac{\partial \Psi}{\partial w}\right|_{\text{SURFACE}} = 0 \quad \text{thus} \quad \left.\Psi\right|_{\text{SURFACE}} = \text{constant.}$$

Since the stream function is zero on the axis of symmetry, which intersects the surface, this boundary condition on the stream function becomes:

$$\left.\Psi\right|_{\text{SURFACE}} = 0. \tag{31}$$

This can be written as:

$$\sum_{n=0}^{\infty} U_n V_n(w) \Big|_{\text{SURFACE}} = 0 \quad \text{or} \quad U_n \Big|_{\text{SURFACE}} = 0,$$

since the Gegenbauer polynomials constitute a complete set and are independent for each n.

In terms of the stream function, boundary condition (27) becomes:

$$\frac{f^2}{a^2 \sin\eta} \left.\frac{\partial \Psi}{\partial \mu}\right|_{\text{SURFACE}} = (1-\sigma)\frac{D}{\rho g} \left.(\overline{\nabla \rho_v} \cdot \bar{\tau})\right|_{\text{SURFACE}}.$$

In bispherical coordinates the direction tangential to the surface is described by the unit vector in the η- direction thus:

$$\left.\frac{\partial \Psi}{\partial \mu}\right|_{\text{SURFACE}} = -K \left.\frac{1-w^2}{f} \frac{\partial \rho_v}{\partial w}\right|_{\text{SURFACE}}$$

where $K = \dfrac{(1-\sigma)Da}{\rho_g}$. From equation (13) the vapor density can be written as:

$$\rho_v = \sqrt{f} \sum_{n=0}^{\infty} \phi_n P_n(w) \text{ so:}$$

$$\frac{\partial \rho_v}{\partial w} = \sqrt{f} \sum_{n=0}^{\infty} \phi_n P_n'(w) - \frac{1}{2\sqrt{f}} \sum_{n=0}^{\infty} \phi_n P_n(w) \text{ where}$$

$P_n'(w) = \partial P_n(w)/\partial w$. This boundary condition therefore becomes:

$$f^{3/2} \frac{\partial \Psi}{\partial n}\Big|_{SURFACE} = K(1-w^2)\left[\frac{1}{2}\sum_{n=0}^{\infty} \phi_n P_n(w) - \cosh\mu \sum_{n=0}^{\infty} \phi_n P_n(w) + w \sum_{n=0}^{\infty} \phi_n P_n'(w)\right]\Big|_{SURFACE}$$

This equation can be expressed in terms of Gegenbauer polynomials by use of the identities:[32, 58]

$$(1-w^2) P_n(w) = \frac{(n+1)(n+2)}{(2n+1)(2n+3)} V_{n+1}(w) - \frac{n(n-1)}{(2n+1)(2n-1)} V_{n-1}(w)$$

$$(1-w^2) P_n'(w) = \frac{n(n+1)}{2n+1} V_n(w) \quad , \text{ and}$$

$$(1-w^2)w - P_n'(w) = \frac{n(n+1)(n-1)}{(2n-1)(2n+1)} V_{n-1}(w) + \frac{n(n+1)(n+2)}{(2n+1)(2n+3)} V_{n+1}(w) \quad .$$

By substituting these identities into the boundary condition equation and simplifying one obtains:

$$f^{3/2} \frac{\partial \Psi}{\partial \mu}\Big|_{SURFACE} = \sum_{n=0}^{\infty} \Phi_n V_n(w)\Big|_{SURFACE} \qquad (32)$$

where $\Phi_n = \frac{K}{2} \frac{n(n+1)}{(2n+1)} \{ \phi_{n+1} + \phi_{n-1} - 2 \phi_n \cosh(\mu) \}$.

Writing the expression for the stream function, equation (28), as

$$f^{3/2} \Psi = \sum_{n=0}^{\infty} U_n V_n(w) \quad ,$$

taking the partial derivative with respect to μ of both sides of this equation, and evaluating the expression at the surface in light of equation (31) one obtains:

$$f^{3/2} \left.\frac{\partial \Psi}{\partial \mu}\right|_{SURFACE} = \left.\sum_{n=0}^{\infty} \frac{\partial}{\partial \mu} U_n \; V_n(w)\right|_{SURFACE} .$$

Using this result the boundary condition for velocity tangential to the surface as expressed by equation (32) becomes

$$\left.\sum_{n=0}^{\infty} \Phi_n \; V_n(w)\right|_{SURFACE} = \left.\sum_{n=0}^{\infty} \frac{\partial U_n}{\partial \mu} \; V_n(w)\right|_{SURFACE} \quad \text{or}$$

$$\Phi_n - \left.\frac{\partial U_n}{\partial \mu}\right|_{SURFACE} = 0 . \tag{33}$$

Evaluating equations (31) and (33) at each particle surface the constants A'_n, B'_n, C'_n and D'_n can each be found for every n. As shown by Stimpson and Jeffery,[32] for cases in which the stream function (28) is a solution to the equations of motion, the force on each sphere becomes:

$$F_1 = \eta\pi 2\sqrt{2}/a \sum_{n=1}^{\infty} (2n+1)(A'_n + B'_n + C'_n + D'_n) \tag{34}$$

for the sphere $\mu = \mu_1$ and

$$F_2 = -\eta\pi 2\sqrt{2}/a \sum_{n=1}^{\infty} (2n+1)(A'_n - B'_n + C'_n - D'_n) \tag{35}$$

for the sphere at $\mu = -\mu_2$.

By evaluating equations (31) and (33) at each particle surface, four independent equations are found from which the four constants

A'_n , B'_n , C'_n , and D_n for each value of n can be determined. Since the constants converge for large values of n, the force can be found to the desired accuracy by terminating the sums in equations (34) and (35) at an appropriate value of n.

The resistance force for two spheres moving parallel to their line of centers[32] and moving perpendicular to their line of centers[40] is found in each case by assuming that the spheres have a given velocity, then calculating the resistance force resulting from this velocity. In the present situation, these results will be used to give the velocities both parallel and perpendicular to the line of centers that are necessary to make the total force in each of these directions zero. For motion parallel to the line of centers the sum of the diffusiophoretic force, the parallel component of the gravitational force, and the resistance force on each particle must be zero. For the motion perpendicular to the line of centers the perpendicular component of the gravitational force and the resistance force on each particle must add up to zero.

For a given two particle system at an arbitrary separation the velocity of each particle can be found from the above analysis. To find the trajectories the particles will be allowed to move at these velocities for an increment of time resulting in a new orientation for which new particle velocities can be found.

IV DISCUSSION OF RESULTS

A. TEMPERATURE AND VAPOR DENSITY PROFILES

The temperature and vapor density profiles for two juxtaposed, growing water droplets of equal radii are shown in figures 2 and 3. Corresponding profiles for unequal droplets were given by Carstens et. al.[56] In both cases the internal droplet temperatures are constant. Since the temperature and vapor density evaluated at the particle surface are related by the condition of thermal equilibrium, it follows that if the droplet temperature is constant the vapor density gradient tangential to the surface and evaluated at the surface is zero.

Some insight into the question of why the internal temperatures of juxtaposed droplets are constant can be found by considering an isolated growing droplet. The internal temperature for an isolated droplet is constant. If external temperature and density gradients are established near the isolated droplet, the internal droplet temperature will remain constant only if the imposed temperature and density gradients satisfy the power balance:

$$\{ LD\overline{\nabla\rho} + K_e \overline{\nabla T} \} \cdot \bar{n} = 0. \tag{36}$$

Thus the total amount of heat released at the surface as a consequence of the externally imposed vapor flow must be carried away by the externally imposed temperature gradient. The temperature and density gradients outside any isolated droplet satisfy equation (36). Thus, if two droplets are juxtaposed and the isolated profiles of each serve as the externally imposed gradients on the other, it

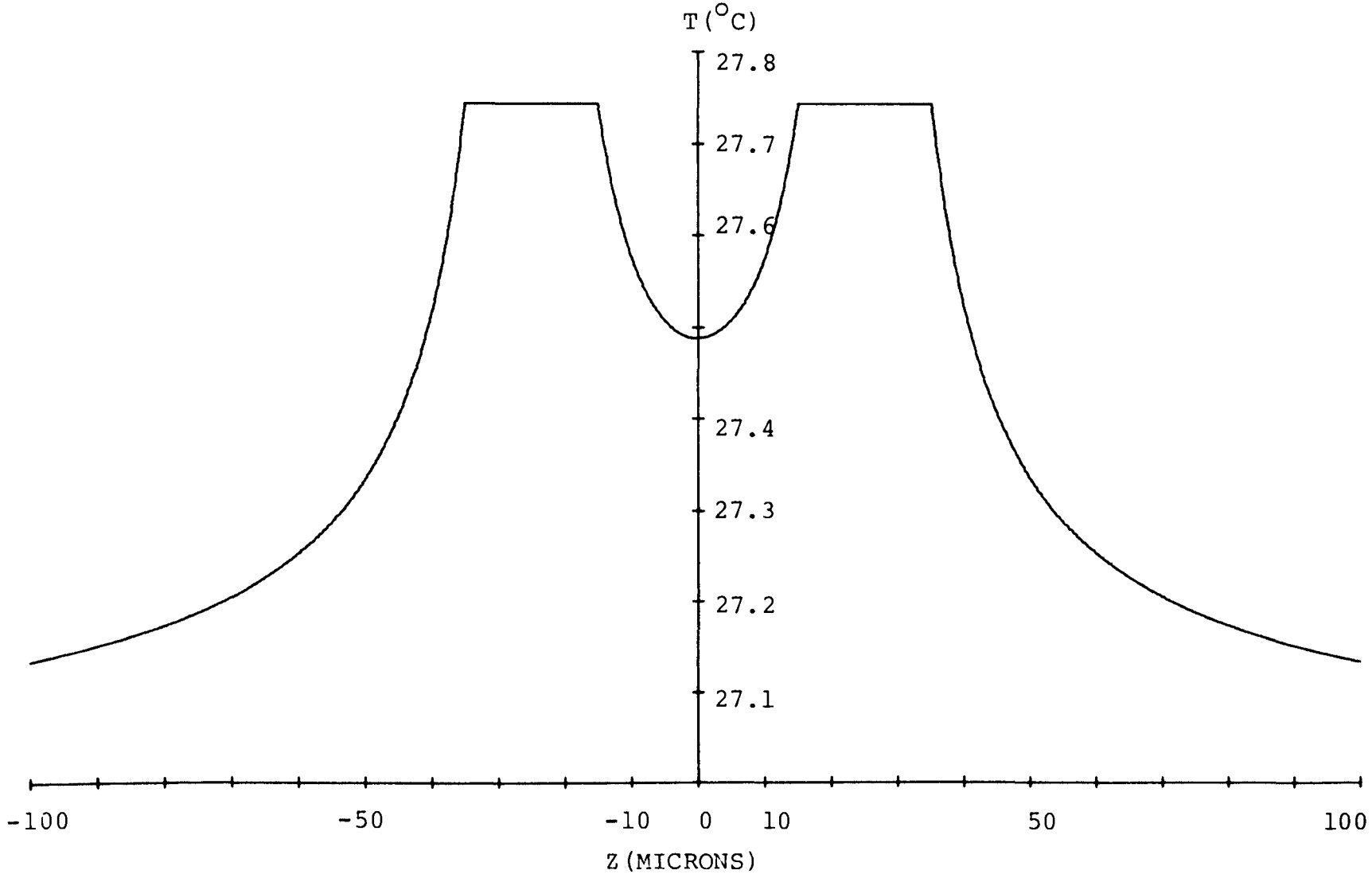

Figure 2. Temperature profile for juxtaposed growing water droplets. Supersaturation is S = 1.05.

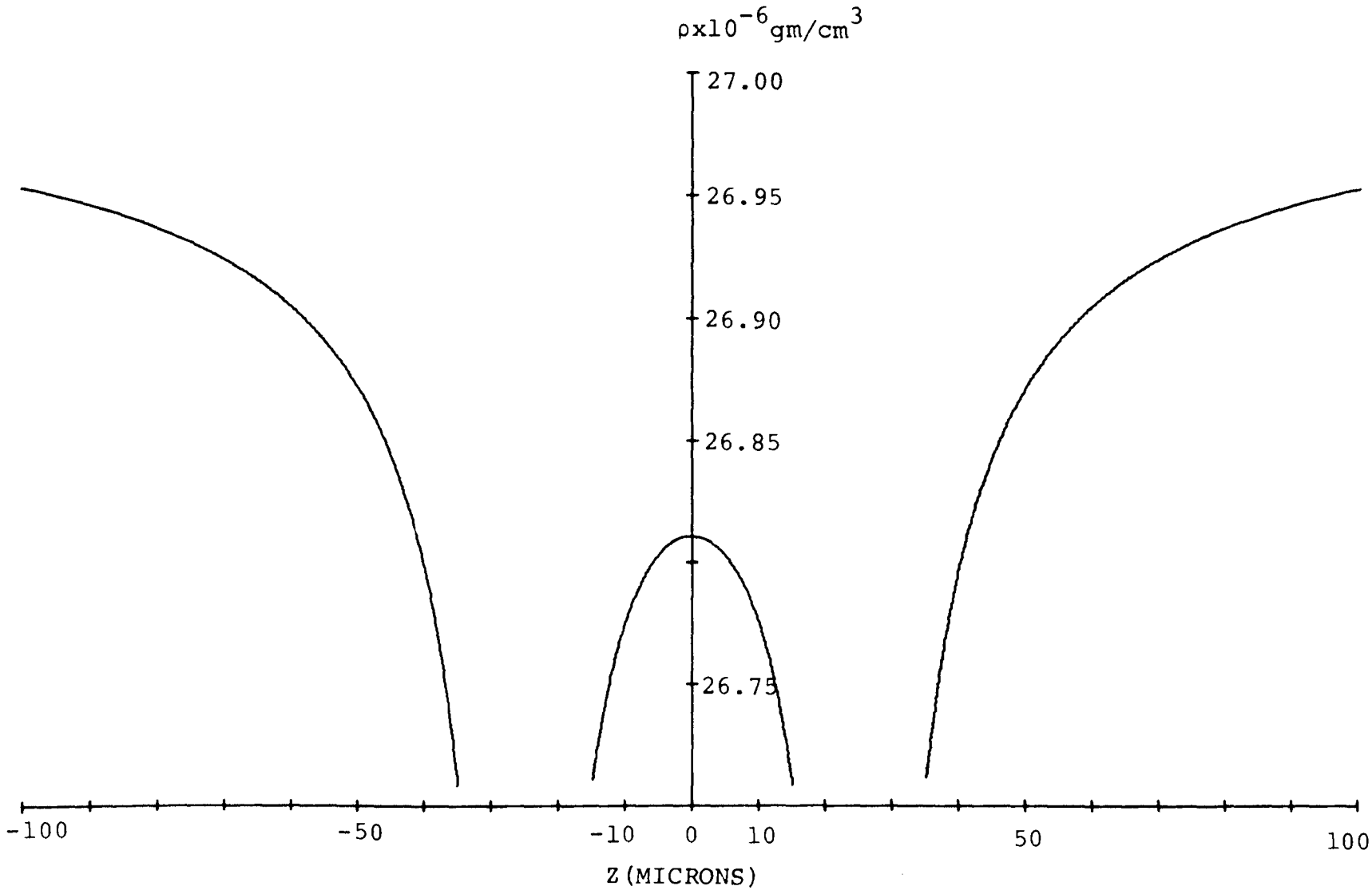

Figure 3. Vapor density profile for juxtaposed growing water droplets. S = 1.05.

is reasonable to expect the internal temperatures to remain constant. Apparently this kind of balance exists in the actual two droplet situation.

Using a similar analysis, consider the juxtaposition of an ice particle and a water droplet, both undergoing diffusional growth. The temperature and vapor density gradients outside an isolated ice particle should satisfy equation (36), where L in this case represents the heat of sublimation. Therefore, at any point outside the isolated ice particle there is a flow of vapor which, if allowed to deposit on an ice surface, would give up an amount of heat that would be totally conducted away by the external temperature gradient existing at that point. However, if a water droplet is placed near the ice particle, the side of the droplet farthest from the ice surface would intercept a vapor flow from the externally imposed density gradient, which upon condensation would give up a smaller amount of heat than is conducted away by the externally imposed temperature gradient, since the latent heat of water is less than the heat of sublimation of ice. This side of the droplet would thus become cooler. The other side of the droplet would be heated since the imposed temperature gradient conducts more heat toward the surface than is lost due to evaporation induced by the externally imposed density gradient. Figure 4 shows the temperature profile for a juxtaposed ice particle and a water droplet. Note that there is a gradient of temperature inside the water droplet and in the sense as suggested. The above analysis indicates

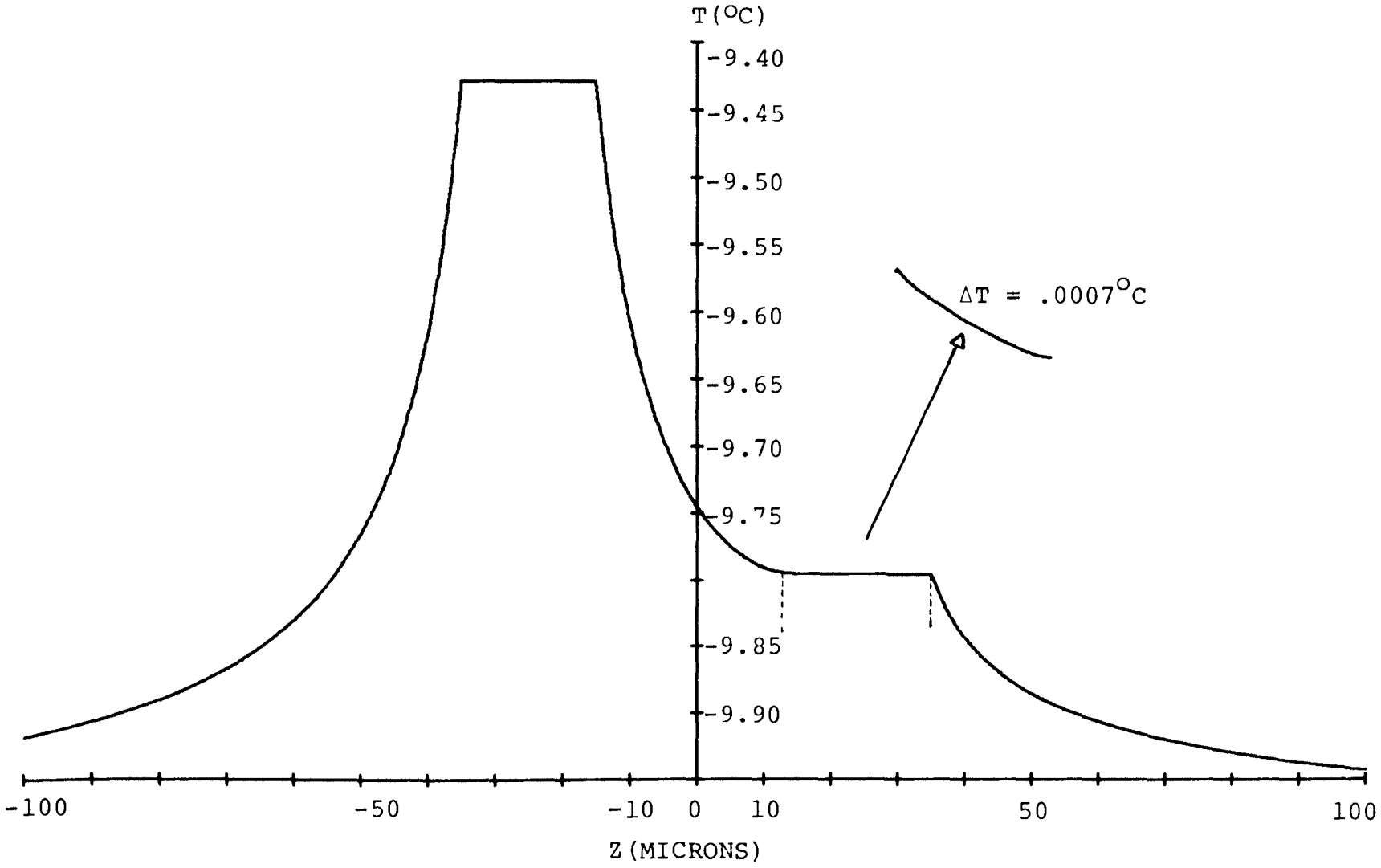

Figure 4. Temperature profile for a juxtaposed water droplet (right) and an ice particle. The supersaturation with respect to the water is 1.05 and with respect to the ice 1.137. The insert shows the internal temperature of the water.

that there should also exist a temperature gradient internal to the ice particle which turns out to be true. However, this gradient is much smaller, partly due to the higher thermal conductivity of ice. Figure 5 shows the corresponding vapor density profile for the ice water juxtaposition.

The temperature and vapor density for a system of ice and an inert particle is shown in figures 6 and 7 respectively. It is apparent from figure 7 that there is a rather large vapor density gradient tangential to the surface of the inert particle. The vapor density gradient tangential to the surface of the ice particle is quite small. The presence of the inert particle significantly affects the profiles near the growing particle. As the particle separation decreases this effect becomes more pronounced, since the inert particle will occupy a greater solid angle, as measured from the center of the ice particle, from which vapor cannot be extracted.

B. DIFFUSIOPHORETIC FORCE

The diffusiophoretic force on each of two juxtaposed growing water droplets is zero. This is true since the velocity field which satisfies boundary conditions (5) and (6) as well as the boundary condition on the velocity far from the droplets, and which is a solution to the equation of motion can be written as:

$$\bar{v} = - \frac{D}{\rho_g} \overline{\nabla \rho_v} .$$

As mentioned previously, this velocity field, to a very good approximation, can be interpreted as the gradient of a scalar function

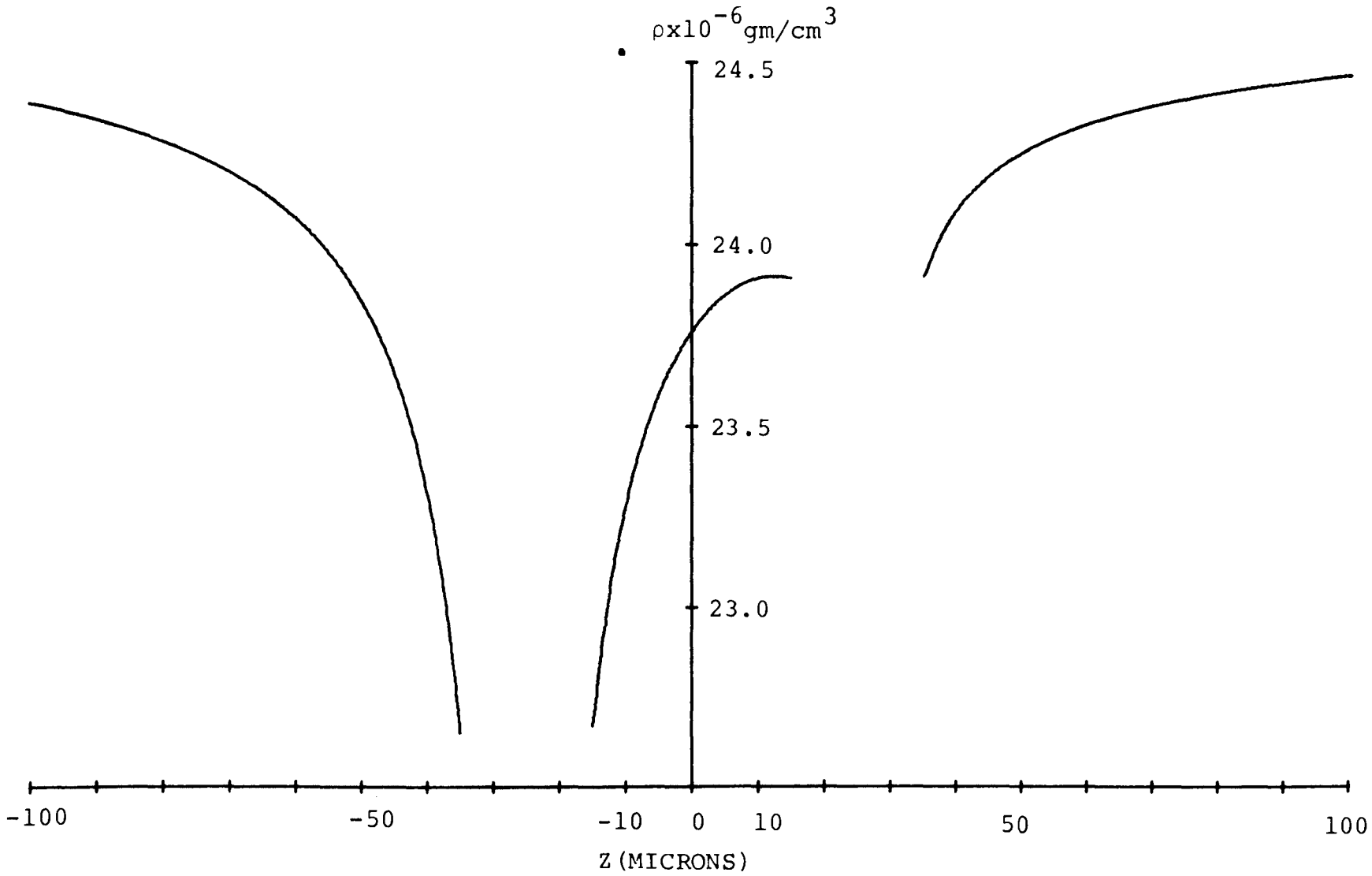

Figure 5. Vapor density profile for a juxtaposed water droplet (Right) and an ice particle. The supersaturation with respect to the water is 1.05 and with respect to the ice 1.135.

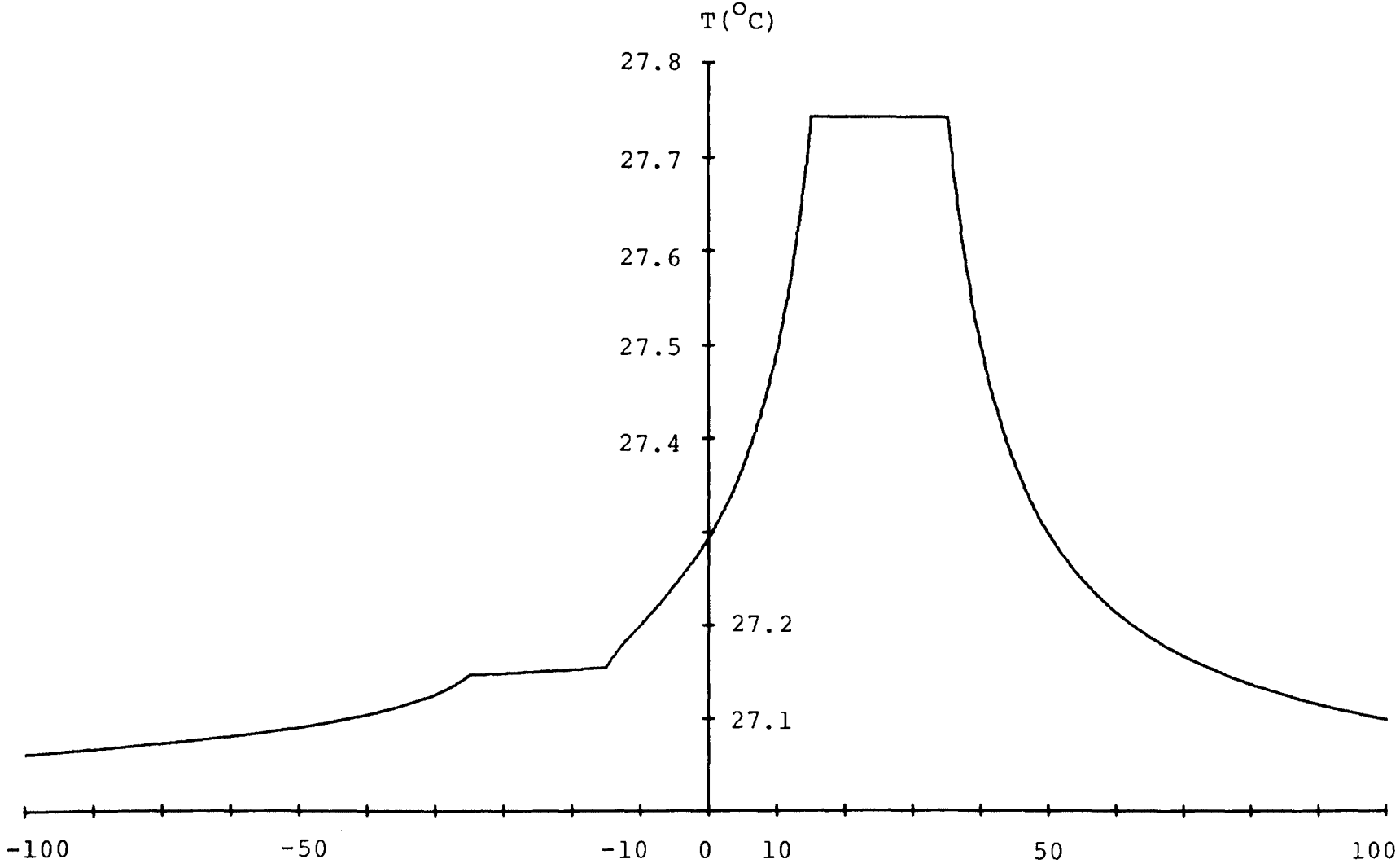

Figure 6. Temperature profile for a juxtaposed water droplet (right) and an ice particle. S = 1.05.

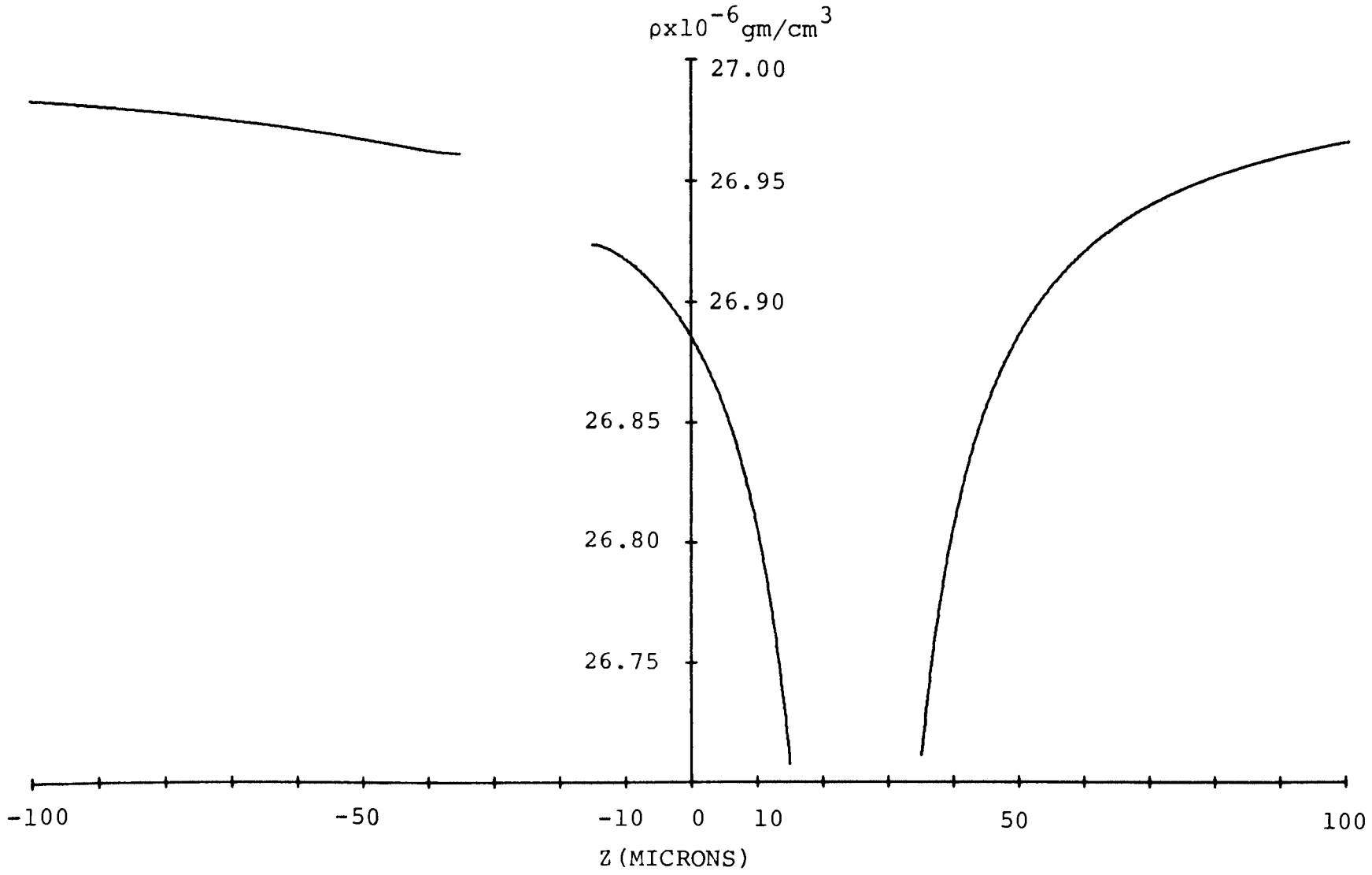

Figure 7. Vapor density profile for a juxtaposed water droplet (right) and an inert particle. S = 1.05.

and, hence, gives a zero force.

That this velocity field satisfies the velocity boundary condition tangential to the droplet surface is true because the internal droplet temperatures are constant. Conversely, if the internal droplet temperature of one of the droplets is not constant, the velocity field cannot be written as the gradient of a scalar unless the slip coefficient is taken as unity which is physically unacceptable.

The diffusiophoretic force on a spherical ice particle of radius 10 microns and an 8 micron water droplet for various separations is given in table I. The spheres are oriented such that the negative force on the ice particle means that it is attracted toward the water droplet. The force on the droplet is such as to repel it from the ice particle. Since the force on the droplet is larger, the overall relative force is repulsive. As the distance between surfaces increases from one to about ten microns the force on each particle decreases by more than an order of magnitude.

At lower supersaturations and small separations the situation may exist where the ice is growing and the water is evaporating. In this case the internal temperature gradient of the ice particle reverses in direction, hence the force reverses in direction. As a result, the force on each particle is such as to repel it from the other.

If the supersaturation is lowered to the point that both the ice and the water are evaporating, the force on the ice particle would be away from the water droplet, but the force on the water droplet would be toward the ice particle. Thus the overall relative

TABLE I

Diffusiophoretic force between an ice particle and a water droplet. F_1 is the force on the ice particle of radius 10 microns and F_2 is the force on the water droplet of radius 8 microns. D is the distance between centers. The supersaturation with respect to the droplet is 1.05 and with respect to the ice 1.137.

D(microns)	F_1(dynes)	F_2(dynes)
0.1900E 02	-0.1184E 00	-0.1268E 00
0.1901E 02	-0.1164E 00	-0.1247E 00
0.1903E 02	-0.1137E 00	-0.1220E 00
0.1911E 02	-0.1038E 00	-0.1121E 00
0.1922E 02	-0.9307E-01	-0.1012E 00
0.1935E 02	-0.8208E-01	-0.9011E-01
0.1952E 02	-0.7145E-01	-0.7932E-01
0.1972E 02	-0.6152E-01	-0.6921E-01
0.1997E 02	-0.5251E-01	-0.6000E-01
0.2026E 02	-0.4449E-01	-0.5177E-01
0.2060E 02	-0.3746E-01	-0.4451E-01
0.2099E 02	-0.3138E-01	-0.3818E-01
0.2146E 02	-0.2616E-01	-0.3271E-01
0.2199E 02	-0.2173E-01	-0.2800E-01
0.2261E 02	-0.1799E-01	-0.2398E-01
0.2331E 02	-0.1484E-01	-0.2055E-01
0.2496E 02	-0.1012E-01	-0.1526E-01
0.2700E 02	-0.6874E-02	-0.1143E-01
0.2946E 02	-0.4648E-02	-0.8648E-02
0.3538E 02	-0.2210E-02	-0.5235E-02
0.4298E 02	-0.1057E-02	-0.3278E-02
0.5216E 02	-0.5178E-03	-0.2132E-02
0.6268E 02	-0.2618E-03	-0.1442E-02
0.7429E 02	-0.1366E-03	-0.1014E-02
0.8673E 02	-0.7314E-04	-0.7396E-03
0.9985E 02	-0.3955E-04	-0.5562E-03

force for situations in which both particles are evaporating would be attractive, since the magnitude of the force on the droplet would still be larger.

The forces on a spherical ice particle and a spherical inert particle for various separations are shown in table II. For this case, the forces are larger than the corresponding values in table I by about two orders of magnitude. The force on the inert particle is larger than that on the ice particle and is toward the ice particle. The force on the ice particle is away from the inert particle. The overall relative force is thus attractive. If the ice particle were evaporating the force on the inert particle would be such as to repel it from the ice making the overall relative force for this case repulsive.

Table III gives the force on a growing water droplet juxtaposed with an inert particle. Qualitatively, these results are identical to the situation shown in table II. Here the relative force is attractive and smaller than if the droplet were replaced by an ice particle, suggesting that ice is a more efficient scavenger than water.

That the diffusiophoretic force on a particle near an ice particle is larger than that force near a water droplet is true because the supersaturation of the bulk medium with respect to the ice surface is considerably larger than the supersaturation as seen from the water surface. Therefore, the flow of vapor toward the ice particle is larger than that toward the water droplet. The Stefan flow near the ice particle and the resulting force on an

TABLE II

Diffusiophoretic force between an ice particle and an inert particle. F_1 is the force on the 8 micron inert particle and F_2 the force on the 10 micron ice particle. D is the distance between centers. The supersaturation with respect to the ice particle is 1.137.

D(microns)	F_1(dynes)	F_2(dynes)
0.1900E 02	0.1036E 02	0.1147E 02
0.1902E 02	0.1019E 02	0.1130E 02
0.1906E 02	0.1000E 02	0.1111E 02
0.1917E 02	0.9430E 01	0.1053E 02
0.1931E 02	0.8787E 01	0.9882E 01
0.1949E 02	0.8097E 01	0.9182E 01
0.1970E 02	0.7378E 01	0.8453E 01
0.1995E 02	0.6651E 01	0.7713E 01
0.2024E 02	0.5933E 01	0.6981E 01
0.2059E 02	0.5238E 01	0.6270E 01
0.2100E 02	0.4581E 01	0.5593E 01
0.2147E 02	0.3969E 01	0.4960E 01
0.2201E 02	0.3411E 01	0.4376E 01
0.2264E 02	0.2909E 01	0.3846E 01
0.2335E 02	0.2464E 01	0.3369E 01
0.2416E 02	0.2075E 01	0.2946E 01
0.2507E 02	0.1738E 01	0.2572E 01
0.2609E 02	0.1451E 01	0.2244E 01
0.2838E 02	0.1012E 01	0.1723E 01
0.3112E 02	0.7029E 00	0.1328E 01
0.3433E 02	0.4877E 00	0.1029E 01
0.4169E 02	0.2465E 00	0.6460E 00
0.5067E 02	0.1290E 00	0.4181E 00
0.6102E 02	0.7106E-01	0.2806E 00
0.7249E 02	0.4136E-01	0.1956E 00
0.8483E 02	0.2540E-01	0.1414E 00
0.9787E 02	0.1637E-01	0.1055E 00

TABLE III

Diffusiophoretic force between a water droplet and an inert particle. F_1 is the force on the 10 micron water droplet and F_2 is the force on the 8 micron inert particle. D is the distance between centers. The supersaturation with respect to the droplet is 1.05.

D(microns)	F_1(dynes)	F_2(dynes)
0.1900E 02	0.4236E 01	0.4665E 01
0.1902E 02	0.4185E 01	0.4613E 01
0.1904E 02	0.4121E 01	0.4549E 01
0.1914E 02	0.3906E 01	0.4331E 01
0.1926E 02	0.3658E 01	0.4081E 01
0.1941E 02	0.3387E 01	0.3807E 01
0.1959E 02	0.3100E 01	0.3517E 01
0.1981E 02	0.2808E 01	0.3220E 01
0.2008E 02	0.2516E 01	0.2923E 01
0.2039E 02	0.2231E 01	0.2633E 01
0.2076E 02	0.1960E 01	0.2355E 01
0.2119E 02	0.1705E 01	0.2093E 01
0.2168E 02	0.1471E 01	0.1850E 01
0.2225E 02	0.1259E 01	0.1628E 01
0.2291E 02	0.1070E 01	0.1427E 01
0.2366E 02	0.9038E 00	0.1249E 01
0.2450E 02	0.7592E 00	0.1090E 01
0.2644E 02	0.5342E 00	0.8362E 00
0.2880E 02	0.3723E 00	0.6422E 00
0.3161E 02	0.2583E 00	0.4953E 00
0.3820E 02	0.1296E 00	0.3077E 00
0.4647E 02	0.6665E-01	0.1963E 00
0.5623E 02	0.3584E-01	0.1296E 00
0.6722E 02	0.2035E-01	0.8891E-01
0.7919E 02	0.1220E-01	0.6326E-01
0.9193E 02	0.7705E-02	0.4657E-01
0.1052E 03	0.5087E-02	0.3532E-01

inert particle is greater than if the ice is replaced by a droplet.

C. FALL TRAJECTORIES

The significance of the diffusiophoretic force in terms of atmospheric processes for the particle sizes considered here can best be determined by comparing the particle trajectories with and without accounting for the diffusiophoretic force. To this end, table IV gives values of orientation and corresponding velocities for a 10 micron sphere falling toward an 8 micron sphere. The initial position was such that the larger sphere would come to within 1 micron separation between surfaces at the point of closest approach. Due to the interference of the flow fields around each sphere, which becomes more pronounced for small separations there is a component of horizontal velocity denoted as V1X and V2X, for each particle, giving the impression that the particles are "sliding along their line of centers." As noted experimentally by Eveson and Hall.[43] As the separation becomes smaller, the velocity of the smaller particle in the horizontal direction increases, in effect moving aside for the larger particle to pass. The vertical velocity of each sphere is larger than the Stokes value for isolated spheres due to the interference of the flow fields. For large sphere separations the fall velocity of each sphere approaches the Stokes value.

The diffusiophoretic force as discussed here is associated with diffusional growth or evaporation processes. A calculation of the trajectories to be accurate should account for changes in radius of

TABLE IV

Values of orientation and instantaneous velocity for two inert spheres.

D = distance between centers.

$\alpha = \mathrm{Tan}^{-1} \frac{\Delta X}{\Delta Z}$ where ΔX and ΔZ are the horizontal and vertical separations respectively of the spheres.

V1X,V1Z = instantaneous velocities of sphere 1 (10 microns) in the X(horizontal) and Z(vertical) directions respectively.

V2X,V2Z = instantaneous velocities of sphere 2(microns) in the X(horizontal) and Z(vertical) directions respectively.

D(microns)	α(degrees)	V1X($^{cm}/_{sec}$)	V1Z($^{cm}/_{sec}$)	V2X($^{cm}/_{sec}$)	V2Z($^{cm}/_{sec}$)
0.1900E 02	0.900E 02	0	-0.1407E 01	0	-0.1258E 01
0.1901E 02	0.877E 02	-0.5896E-02	-0.1408E 01	-0.1064E-01	-0.1258E 01
0.1903E 02	0.854E 02	-0.1159E-01	-0.1409E 01	-0.2111E-01	-0.1259E 01
0.1911E 02	0.809E 02	-0.2175E-01	-0.1413E 01	-0.4079E-01	-0.1263E 01
0.1922E 02	0.764E 02	-0.3032E-01	-0.1418E 01	-0.5871E-01	-0.1268E 01
0.1936E 02	0.719E 02	-0.3735E-01	-0.1424E 01	-0.7461E-01	-0.1275E 01
0.1952E 02	0.674E 02	-0.4301E-01	-0.1430E 01	-0.8834E-01	-0.1284E 01
0.1973E 02	0.630E 02	-0.4751E-01	-0.1436E 01	-0.9982E-01	-0.1292E 01
0.1997E 02	0.586E 02	-0.5098E-01	-0.1442E 01	-0.1089E 00	-0.1302E 01
0.2026E 02	0.544E 02	-0.5351E-01	-0.1447E 01	-0.1156E 00	-0.1311E 01
0.2060E 02	0.503E 02	-0.5512E-01	-0.1452E 01	-0.1200E 00	-0.1319E 01

Con't next page

Table IV Con't.

D(microns)	α (degrees)	V1X($^{cm}/_{sec}$)	V1Z($^{cm}/_{sec}$)	V2X($^{cm}/_{sec}$)	V2Z($^{cm}/_{sec}$)
0.2100E 02	0.463E 02	-0.5583E-01	-0.1457E 01	-0.1219E 00	-0.1327E 01
0.2146E 02	0.426E 02	-0.5571E-01	-0.1460E 01	-0.1217E 01	-0.1332E 01
0.2200E 02	0.391E 02	-0.5482E-01	-0.1463E 01	-0.1196E 00	-0.1336E 01
0.2261E 02	0.358E 02	-0.5328E-01	-0.1465E 01	-0.1159E 00	-0.1337E 01
0.2332E 02	0.327E 02	-0.5120E-01	-0.1465E 01	-0.1109E 00	-0.1336E 01
0.2497E 02	0.272E 02	-0.4590E-01	-0.1463E 01	-0.9827E-01	-0.1326E 01
0.2701E 02	0.225E 02	-0.3983E-01	-0.1456E 01	-0.8410E-01	-0.1308E 01
0.2948E 02	0.187E 02	-0.3370E-01	-0.1445E 01	-0.7012E-01	-0.1281E 01
0.3539E 02	0.131E 02	-0.2283E-01	-0.1418E 01	-0.4639E-01	-0.1219E 01
0.4300E 02	0.948E 01	-0.1499E-01	-0.1386E 01	-0.2995E-01	-0.1152E 01
0.5219E 02	0.713E 01	-0.9863E-02	-0.1356E 01	-0.1951E-01	-0.1090E 01
0.6271E 02	0.558E 01	-0.6644E-02	-0.1330E 01	-0.1307E-01	-0.1038E 01
0.7432E 02	0.450E 01	-0.4624E-02	-0.1309E 01	-0.9075E-02	-0.9968E 00
0.8677E 02	0.374E 01	-0.3331E-02	-0.1292E 01	-0.6525E-02	-0.9639E 00
0.9988E 02	0.317E 01	-0.2477E-02	-0.1279E 01	-0.4848E-02	-0.9378E 00

growing or evaporating particles. This effect on the trajectories will be neglected, so that any differences in trajectories will correspond to diffusiophoretic forces.

Table V gives the relative orientation and velocities for a spherical ice particle of radius 10 microns falling toward a growing water droplet of radius 8 microns. Again, the initial positions are such that when the particle centers lie on the same horizontal plane, the surfaces are separated by 1 micron. It is apparent from comparison of the corresponding instantaneous velocities in tables IV and V that the effect of diffusiophoresis on the motion is not appreciable.

Values of relative orientation and instantaneous velocities for a 10 micron spherical ice particle and an 8 micron inert particle are shown in table VI. Comparing these values to the corresponding values in table IV, it appears that the diffusiophoretic force does noticeably influence the trajectories. The effect is most apparent for orientations in which the particles are positioned near the same horizontal plane, corresponding to $\alpha = 90^{o}$. For this orientation the horizontal force, derived from the interference of the flow fields around two settling spheres, is at its smaller values and due to the close proximity of the spheres the diffusiophoretic force is at its maximum value.

A plot of the relative position of the particles during the trajectory for the ice and inert particle interaction is shown in curve B of figure 8. For comparison, the corresponding plot for two inert spheres is given in curve A. Defining an impact parameter,

TABLE V

Values of orientation and instantaneous velocity for a 10 micron ice particle (sphere 1) falling toward an 8 micron water droplet. (See Table IV for explanation of symbols.) The supersaturation with respect to the water is 1.05 and with respect to the ice 1.137.

D(microns)	α (degrees)	V1X($^{cm}/_{sec}$)	V1Z($^{cm}/_{sec}$)	V2X($^{cm}/_{sec}$)	V2Z($^{cm}/_{sec}$)
0.1900E 02	0.900E 02	-0.6000E-03	-0.1407E 01	-0.6309E-03	-0.1258E 01
0.1901E 02	0.877E 02	-0.6485E-02	-0.1408E 01	-0.1126E-01	-0.1258E 01
0.1903E 02	0.854E 02	-0.1217E-01	-0.1409E 01	-0.2172E-01	-0.1259E 01
0.1911E 02	0.809E 02	-0.2228E-01	-0.1413E 01	-0.4134E-01	-0.1263E 01
0.1922E 02	0.764E 02	-0.3079E-01	-0.1419E 01	-0.5920E-01	-0.1268E 01
0.1935E 02	0.719E 02	-0.3775E-01	-0.1424E 01	-0.7504E-01	-0.1275E 01
0.1952E 02	0.674E 02	-0.4335E-01	-0.1430E 01	-0.8871E-01	-0.1284E 01
0.1972E 02	0.630E 02	-0.4779E-01	-0.1436E 01	-0.1001E 00	-0.1293E 01
0.1997E 02	0.586E 02	-0.5121E-01	-0.1442E 01	-0.1092E 00	-0.1302E 01
0.2026E 02	0.544E 02	-0.5369E-01	-0.1447E 01	-0.1158E 00	-0.1311E 01
0.2060E 02	0.503E 02	-0.5526E-01	-0.1452E 01	-0.1201E 00	-0.1319E 01
0.2099E 02	0.463E 02	-0.5595E-01	-0.1457E 01	-0.1221E 00	-0.1327E 01
0.2146E 02	0.426E 02	-0.5580E-01	-0.1460E 01	-0.1218E 00	-0.1332E 01
0.2199E 02	0.391E 02	-0.5489E-01	-0.1463E 01	-0.1197E 00	-0.1336E 01
0.2261E 02	0.358E 02	-0.5333E-01	-0.1465E 01	-0.1160E 00	-0.1337E 01
0.2331E 02	0.327E 02	-0.5125E-01	-0.1465E 01	-0.1109E 00	-0.1336E 01
0.2496E 02	0.272E 02	-0.4592E-01	-0.1463E 01	-0.9831E-01	-0.1326E 01
0.2700E 02	0.225E 02	-0.3985E-01	-0.1456E 01	-0.8413E-01	-0.1308E 01
0.2946E 02	0.187E 02	-0.3371E-01	-0.1445E 01	-0.7015E-01	-0.1282E 01
0.3538E 02	0.131E 02	-0.2284E-01	-0.1418E 01	-0.4640E-01	-0.1219E 01
0.4298E 02	0.947E 01	-0.1499E-01	-0.1386E 01	-0.2996E-01	-0.1152E 01
0.5216E 02	0.713E 01	-0.9865E-02	-0.1356E 01	-0.1952E-01	-0.1090E 01
0.6268E 02	0.557E 01	-0.6644E-02	-0.1330E 01	-0.1807E-01	-0.1038E 01
0.7429E 02	0.450E 01	-0.4624E-02	-0.1309E 01	-0.9075E-02	-0.9969E 00
0.8673E 02	0.374E 01	-0.3330E-02	-0.1292E 01	-0.6525E-02	-0.9640E 00
0.9985E 02	0.317E 01	-0.2476E-02	-0.1279E 01	-0.4847E-02	-0.9379E 00

TABLE VI

Values of orientation and relative velocity for a 10 micron ice particle (sphere 1) falling toward an 8 micron inert particle. (See Table IV for an explanation of the symbols.) The supersaturation with respect to the ice particle is 1.137.

D(microns)	α (degrees)	V1X($^{cm}/_{sec}$)	V1Z($^{cm}/_{sec}$)	V2X($^{cm}/_{sec}$)	V2Z($^{cm}/_{sec}$)
0.1900E 02	0.9000E 02	0.5335E-01	-0.1407E 01	0.5627E-01	-0.1258E 01
0.1902E 02	0.8775E 02	0.4655E-01	-0.1406E 01	0.4474E-01	-0.1256E 01
0.1906E 02	0.8549E 02	0.3981E-01	-0.1406E 01	0.3321E-01	-0.1254E 01
0.1917E 02	0.8096E 02	0.2647E-01	-0.1406E 01	0.1026E-01	-0.1253E 01
0.1931E 02	0.7640E 02	0.1414E-01	-0.1408E 01	-0.1159E-01	-0.1255E 01
0.1949E 02	0.7183E 02	0.2809E-02	-0.1411E 01	-0.3198E-01	-0.1258E 01
0.1970E 02	0.6728E 02	-0.7520E-02	-0.1415E 01	-0.5055E-01	-0.1264E 01
0.1995E 02	0.6278E 02	-0.1680E-01	-0.1419E 01	-0.6694E-01	-0.1270E 01
0.2024E 02	0.5838E 02	-0.2493E-01	-0.1424E 01	-0.8081E-01	-0.1278E 01
0.2059E 02	0.5409E 02	-0.3179E-01	-0.1430E 01	-0.9190E-01	-0.1286E 01
0.2100E 02	0.4997E 02	-0.3727E-01	-0.1435E 01	-0.1000E 00	-0.1294E 01
0.2147E 02	0.4602E 02	-0.4134E-01	-0.1440E 01	-0.1053E 00	-0.1301E 01
0.2201E 02	0.4227E 02	-0.4405E-01	-0.1444E 01	-0.1079E 00	-0.1307E 01
0.2264E 02	0.3874E 02	-0.4550E-01	-0.1447E 01	-0.1081E 00	-0.1310E 01
0.2335E 02	0.3544E 02	-0.4585E-01	-0.1450E 01	-0.1062E 00	-0.1312E 01
0.2416E 02	0.3238E 02	-0.4529E-01	-0.1451E 01	-0.1027E 00	-0.1310E 01
0.2507E 02	0.2955E 02	-0.4398E-01	-0.1450E 01	-0.9795E-01	-0.1306E 01
0.2609E 02	0.2695E 02	-0.4212E-01	-0.1449E 01	-0.9227E-01	-0 1299E 01
0.2838E 02	0 2241E 02	-0.3728E-01	-0.1443E 01	-0.7948E-01	-0 1280E 01
0.3112E 02	0 1869E 02	-0.3188E-01	-0.1432E 01	-0 6650E-01	-0 1254E 01
0 3433E 02	0 1569E 02	-0.2661E-01	-0.1419E 01	-0 5454E-01	-0.1223E 01
0.4169E 02	0.1129E 02	-0.1782E-01	-0.1389E 01	-0.3573E-01	-0.1158E 01
0.5067E 02	0.8459E 01	-0.1180E-01	-0.1359E 01	-0.2336E-01	-0.1096E 01
0.6102E 02	0.6579E 01	-0.7954E-02	-0.1333E 01	-0.1563E-01	-0.1044E 01
0.7249E 02	0.5291E 01	-0.5521E-02	-0.1311E 01	-0.1081E-01	-0.1001E 01
0.8483E 02	0.4376E 01	-0.3963E-02	-0.1294E 01	-0.7746E-02	-0.9678E 00
0.9787E 02	0.3703E 01	-0.2936E-02	-0.1280E 01	-0.5733E-02	-0.9409E 00

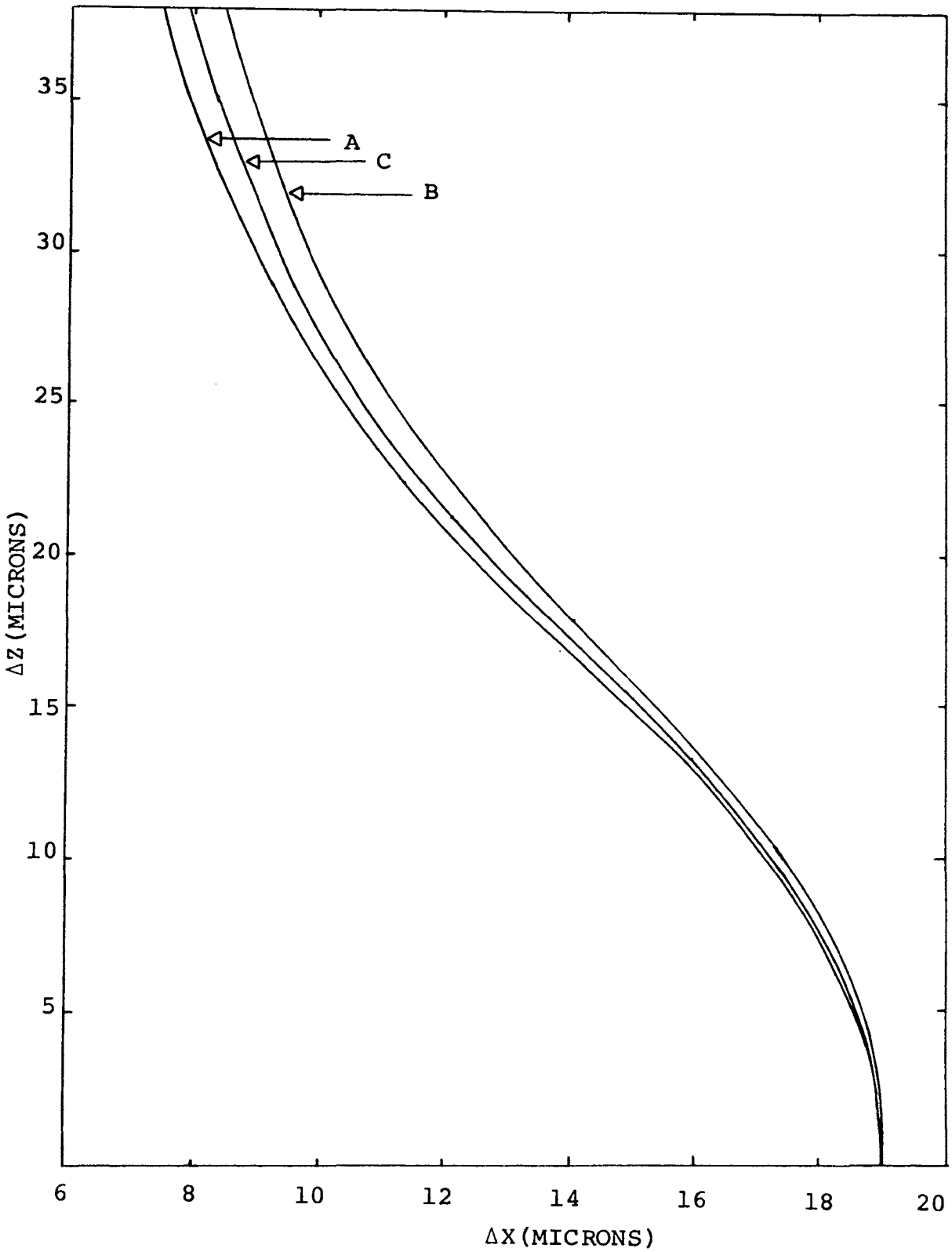

Figure 8. Fall trajectories for 8 and 10 micron spheres. Curve A represents two inert spheres, Curve B an ice and an inert particle and Curve C a water droplet and an inert particle. The supersaturation with respect to water is 1.05 and with respect to ice 1.137.

b, as the horizontal separation of the sphere centers at the beginning of a trajectory that results in a one micron miss, it appears that the diffusiophoretic force for a 10 micron ice particle and an 8 micron inert particle increases the impact parameter by about 1 micron.

Curve C of figure 8 gives the relative trajectory corresponding to a 10 micron growing water droplet falling toward an 8 micron inert particle and missing by 1 micron. The diffusiophoretic force does not change the trajectories as much for this situation as for the ice and inert particle trajectory. The phoretic force increases the impact parameter by about .5 microns.

Curve B of figure 9 shows the trajectory for a 10 micron growing ice particle and a 9.5 micron inert sphere. Shown in curve A is the corresponding trajectory for two inert spheres. Since the spheres are more nearly equal in size than the situation shown in figure 8, the relative fall velocity is smaller and the spheres spend more time in close proximity. As a result the phoretic force has a greater influence on the motion. For this situation the impact parameter is increased by 1.5 microns due to diffusiophoresis.

Recent calculations for collision efficiencies of small spheres falling under the assumptions of creeping, steady motion are given by Sartor and Davis[36] (1967). They defined the collision efficiency as $E = b^2/(R_1 + R_2)^2$ where b is the impact parameter for a grazing collision and R_1 , R_2 the radii of the spheres. As mentioned earlier, the sphere surfaces are not permitted to touch in the present calculation. (The same criticisms can, of course, be made concerning

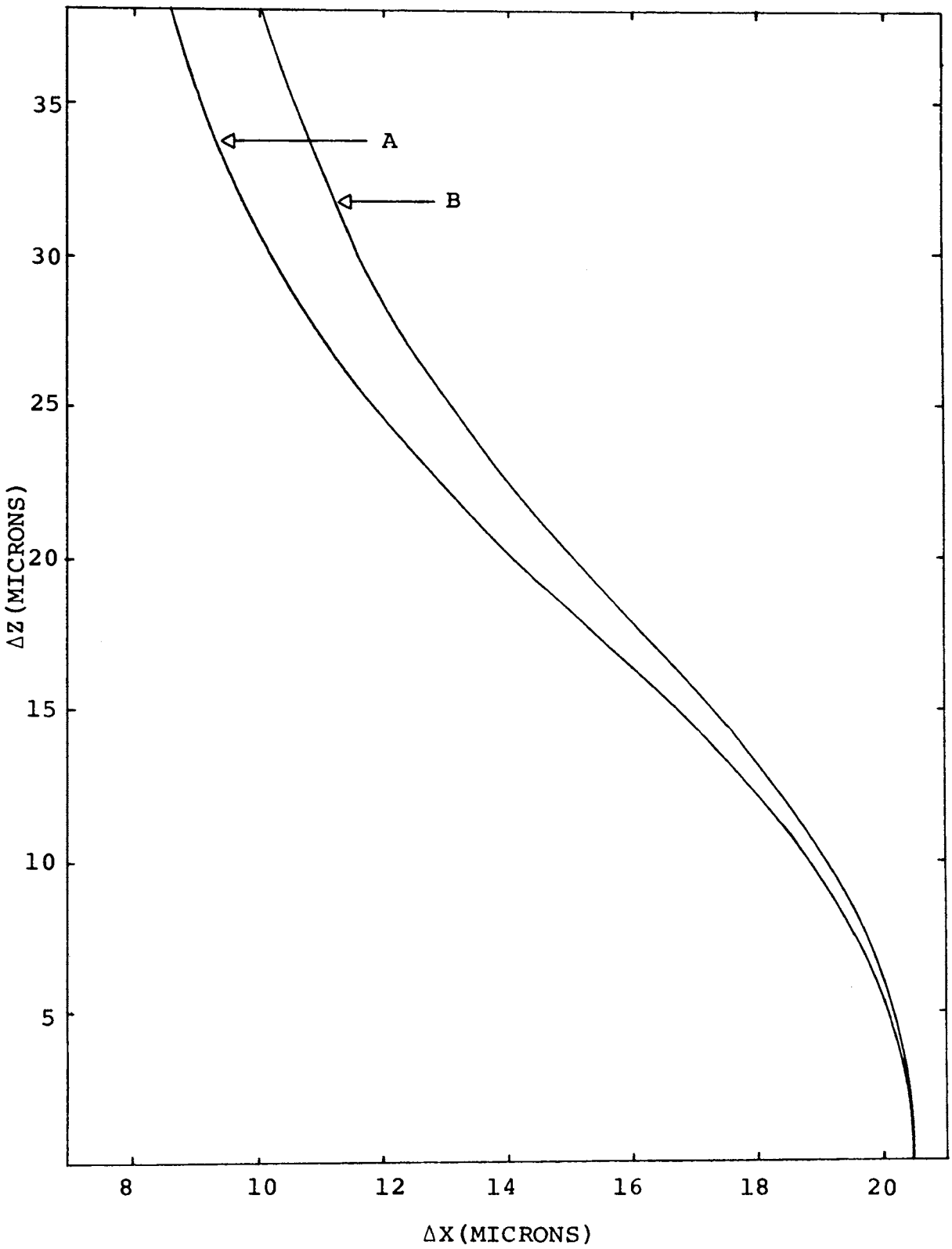

Figure 9. Fall trajectories for 9.5 and 10 micron spheres. Curve A corresponds to two inert spheres and curve B to an ice particle and an inert sphere. The supersaturation with respect to the ice is 1.135.

the Sartor and Davis calculations.) However, using the values of collision efficiencies given by Sartor and Davis and assuming that the changes in the impact parameters mentioned above due to diffusiophoresis apply to a grazing collision as well, one can get an idea of how diffusive forces change the impact parameters.

In the spirit of these assumptions, the impact parameter for a growing 10 micron ice sphere falling toward an 8 micron inert particle is increased by a factor of 1.4 due to diffusive forces. If the inert particle is increased in size to 9.5 microns the diffusive forces increase the impact parameter by a factor of 1.7.

Judging from curve C of figure 8 it appears that diffusive forces for the case of a 10 micron growing water droplet falling toward an 8 micron inert particle increases the impact parameter by a factor of 1.2.

V. APPLICATIONS AND SUGGESTIONS FOR FURTHER STUDY

Although the question as to what value to use for the diffusion slip coefficient is not known precisely, it does not appear to be a limiting factor in judging the significance of the phoretic force. The value for the slip coefficient as used in the tangential velocity boundary condition, equation (27), was $\sigma = .2$. For $\sigma = 1$ the force is zero. This corresponds to perfect slip at the particle surface. In the case of $\sigma = 0$ the force attains its maximum value.

A. ACCRETION AND IN-CLOUD SCAVENGING

The possibility of employing the above calculation for explaining problems involving cloud development does not look encouraging. Droplet growth due to accretion is not affected at all by the phoretic force. Even the number of collisions of water droplets with ice particles do not appear to be significantly enhanced by diffusiophoresis. These results are borne out by field observations of Rosinski[59] (1967) who concluded that "9 - 11 micron diameter cloud droplets will not be removed effectively by phoretic forces."

There does not appear to be sufficient experimental evidence to determine the effect of diffusiophoretic forces on the scavenging of inert particles of several microns radius by droplets or ice particles. The small amount of data presented by Rosinski[59] shows that the concentration of 9-11 micron diameter particles in air is about one-tenth and in ice about one-hundredth of that of 1.5 - 3 micron diameter particles. This data also indicates that the removal of 9-11 micron

diameter particles is independent of the type of ice phase. (One ice phase results from the accretion of supercooled droplets, the other from growth by sublimation.) Since the data points are scattered and include coagulation probabilities in addition to collision efficiencies, the above predictions concerning the enhancement of collision efficiencies of inert particles cannot be tested.

A very difficult problem related to the present discussion is that of the sticking together or coagulation of the particles after collision. If a diffusiophoretic force exists between particles, it may have an influence on the coagulation problem as well as the trajectories. Unfortunately, the diffusiophoretic forces calculated here are not reliable for very close sphere separations. However, these results do suggest that the phoretic force is large for small separations. For cases when the force is attractive, it may increase the chances of coagulation after the spheres collide.

The present study indicates that the diffusiophoretic force may enhance collisions between growing cloud elements and inert particles. The above results could be used to determine the extent of this increase. Such a calculation should necessarily take into account the number distributions of growing cloud elements and inert particles as well as the corresponding size distributions. The number distribution of inert particles is particularly complicated, since the possibility exists that any such particle may serve as a site of condensation of water vapor, thus becoming, in essence, a water droplet or ice particle.

The calculations presented here for the temperature and vapor

density profiles were done assuming that the velocity of each sphere relative to the surrounding medium was small enough that ventilation did not affect the density profiles. For particles of radius greater than about 20 microns, the fall velocity can affect the profiles.[60] Such a drop falling in a supersaturated atmosphere would experience an increase in the vapor density gradient on the front side. This increase in the gradient would increase the diffusiophoretic force on any particle that may be in the path of the falling drop. The result could be an enhancement of the collision efficiency.

Another very important item concerning the calculations presented here is the value of the bulk temperature of the medium. The equilibrium vapor pressure over ice at - 12° C is much lower than that over water at the same temperature making the supersaturation over ice much larger than that over water. The difference between vapor pressures over ice and supercooled water is a function of temperature, being zero at 0° C and increasing to a maximum at - 12° C.[61] The difference in vapor pressures decreases almost linearly from -15° C to near -40° C. (At this temperature most of the supercooled droplets would be frozen.) There is, therefore, a limited temperature range in which the ice particles are more efficient at attracting inert particles than water droplets.

B. LIMITATIONS OF BISPHERICAL GEOMETRY

Another situation that can possibly be exploited by the calculations presented here is the diffusiophoretic force between ice crystals (not spherical) and either droplets or inert particles.

This suggestion is based on calculations by Podzimek[27] which show that the density profile around an ice crystal of complicated shape has nearly the same density profile as around a sphere. This is true since at large distances from the ice crystal the vapor density must necessarily reach the same bulk value as around the spherical ice particle. Also at close distances, any sharp point on the ice crystal would grow faster than a flat surface thus having a large effect on the profile in that region. Since the density profile around a sharp point has nearly spherical geometry, the density profile in the neighborhood of the ice crystal may be very similar to that around an ice sphere.

The effect of the diffusiophoretic force between an ice crystal of complicated geometry and an inert particle or a water droplet should be judged from the effect of the phoretic force on the fall trajectory. Unfortunately the fall trajectory for juxtaposed spheres does not appear to be of much use in this calculation, since the flow field around an ice crystal depends to a large extent on its shape.

Another application of the results presented here could be to give a guideline as to which situations it is necessary to use the relatively complicated bispherical geometry. If one is interested in the temperature and vapor density profiles in the vicinity of two widely spaced droplets, it may be possible to assume that one droplet is suspended in a medium on which is imposed constant, external temperature and vapor density gradients as was done by

Dukhin and Deryagin[12] Accuracy of such a calculation or the diffusiophoretic force resulting from the calculation could be checked using the above results. Depending upon the amount of error one is willing to accept, there is a particle separation greater than which this approximation would be very useful.

C. SCAVENGING OF SUB-MICRON PARTICLES

The calculations presented here for the temperature and vapor density profiles for an ice particle juxtaposed with a water droplet and their relative trajectories could prove useful for the description of the scavenging of sub-micron particles in mixed clouds. Vittori and Prodi[28] (1967) suggested that the capture efficiency of small aerosol particles by ice crystals would be enhanced by the presence of supercooled droplets since the particles would be driven away from the evaporating droplet and toward the growing ice crystal by diffusiophoresis. Rosinski[30] (1967) concluded from field experiments that there is indeed an enhanced scavenging mechanism in mixed clouds for particles of 1.5 - 3 microns in diameter. Slinn and Hales[23,24] have suggested that the particles are scavenged by the water droplets, since for these small particles thermophoresis dominates diffusiophoresis and is in the opposite direction.

If the aerosol particles are considered small enough that their presence does not affect the vapor density and temperature profiles calculated here for a juxtaposed ice particle and water droplet system, then these profiles could be used to calculate the motion of the aerosol particles. The settling motion of the ice

particle and water droplet due to gravity must be taken into account for such a calculation. One would also be wise to consider the distributions of the particles involved to see if such a three-particle interaction is statistically probable before undertaking the calculation.

VI CONCLUSIONS

The diffusiophoretic force between two juxtaposed spherical water droplets is zero. Therefore, the trajectories of the two droplets when falling in a gravitational field are not influenced by the diffusive forces.

The diffusiophoretic force between a spherical ice particle and a spherical water droplet each of which is undergoing diffusional growth or evaporation is non-zero. However, if the sphere sizes are such that ventilation does not disturb the vapor density profiles and the hydrodynamic assumptions of steady, creeping motion are good, the diffusive forces acting between the spheres are not large enough to significantly change the trajectories.

If one of the spheres is a water droplet or spherical ice particle growing by diffusion and the other sphere represents an inert particle, the fall trajectories are influenced in favor of collision. The effect is greatest for the situation in which the spheres are of nearly equal size, since the relative velocities are then small and the spheres can spend more time in close proximity. The magnitude of the force depends on the supersaturation, being larger for higher supersaturations.

VII BIBLIOGRAPHY

1. Davis, M. H. "Collisions of Very Small Cloud Droplets," J. of Geophysical Research, 71, 3101 (1966).

2. Stefan, J., Wein Ber., 83, 943 (1881).

3. Hidy, G. M. and Brock, J. R., The Dynamics of Aerocollidal Systems, Pergamon Press Inc. (1970).

4. Kramers, H. A. and Kistemaker, J., "On the Slip of a Diffusing Gas Mixture Along a Wall," Physica, 10, 699 (1943).

5. Atkin, J., Transactions of the Royal Society Edinb., 32 (1883).

6. Watson, H., Transactions of the Faraday Society, 32, 1073 (1936).

7. Facy, L., Arch. Metero. Geophys. Bioklim., 8A, 269 (1955).

8. Facy, L., C. R. Acad. Sci., Paris, 246, 102, 3161 (1958).

9. Facy, L., Geof. Pura e Appl., 40, No. 2, (1958).

10. Deryagin, B. and Dukhin, S., Dokl. Akad. Nauk SSSR, 111, 613 (1956).

11. Deryagin, B. and Dukhin, S., Dokl. Akad. Nauk SSSR, 106, 851 (1956).

12. Dukhin, S. and Deryagin, B., "A Theory of Interaction between Evaporating or Growing Droplets at Large Distances," Dokl. Akad. Nauk SSSR, 112, 407 [Soviet Physics Doklady, 2, 41 (1957) (English Translation)].

13. Waldmann, L., "On the Motion of Spherical Particles in Non-Homogeneous Gases" in Rarefied Gas Dynamics, ed. L. Talbot, Academic Press, New York, 323 (1961).

14. Waldmann, L. and Schmitt, K. H., "Thermophoresis and Diffusiophoresis of Aerosols" in Aerosol Science, ed. C. N. Davies, Academic Press, New York (1967).

15. Schmitt, K. H., and Waldmann, L., Z Naturforschg, 15d, 843 (1960).

16. Schmitt, K. H., "Untersudnungen an Schwebstoffteilchen in Diffundierendem Wasserdamph," Z. Naturforschg., 16a, 144 (1961).

17. Brock, J. R., "Forces on Aerosols in Gas Mixtures," J. of Colloid Science, 18, 489-501 (1963).

18. Deryagin, B. V., Yalamov, Y. I. and Storozhilova, A. I., "Diffusiophoresis of Large Aerosol Particles," J. of Colloid and Interface Science," 22, 117-125 (1966).

19. Deryagin, B. V. and Yalamov, "Theory of Motion of Large Volatile Particles in Diffusing Gas Mixtures, Soviet Physics - Doklady, 12, 587 (1967).

20. Deryagin, B. V. and Yalamov, "The Theory of the Motion of Solution Drops in a Diffusing Gas Mixture," Soviet Physics - Doklady, 12 (1968).

21. Prokhorov , P. S. and Lenov, L. F., "Investigation of Long - Range Diffusion Forces Between Water Droplets and Non-Volatile Particles," Discussions of the Farady Society, 30, 124 (1960).

22. Waldmann, L., Z. Naturforschg., 30, 124-129 (1961).

23. Slinn, W. G. N. and Hales, J. M., "Phoretic Forces in Scavenging," Proceedings of a Symposium on Precipitation Scavenging, Richland, Washington, June 2 - 9, 1970, National Technical Information Service, U.S. Dept. of Commerce, CONF. - 700601.

24. Slinn, W. G. N. and Hales, J. M., "A Reevaluation of the Role of Thermophoresis as a Mechanism of In-and Below-Cloud Scavenging," J. Atmos. Sci. 8, 1465 (1971).

25. Goldsmith, P., Delafield, H. J and Cox, L. C.,"The Role of Diffusiophoresis in the Scavenging of Radioactive Particles From the Atmosphere," Q. J. R. Met. Soc., 89, 43 (1963).

26. Goldsmith, P. and May, F. G., "Diffusio-and Thermophoresis in Water Vapor Systems," in Aerosol Science, ed. C. N. Davies, Academic Press, New York, (1966).

27. Podzimek, J., "L'Influence Du Courant De Stefan Sur La Capture Des Particles D'AgI Sur Les Elements De Nuage," Journal De Recherches Atmospherigues, 19 (1965).

28. Vittori, O. A., and Prodi, V., "Scavenging of Atmospheric Particles by Ice Crystals," J. Atmos. Sci., 24, 533 (1967).

29. Vittori, O. A. and Prodi, V., "Particle-Free Space in Stefan Flow," Proceedings of a Symposium on Precipitation Scavenging, Richland, Washington, June 2-9, 1970, National Technical Information Service, U.S. Dept. of Commerce, CONF-700601.

30. Rosinski, J., "Insoluble Particles in Hail and Rain," J. Applied Meteorolgy, 6, 1066 (1967).

31. Hocking, L. M., Ph.D Dissertation, University of London, (1958) Unpublished.

32. Stimson, M., and Jeffery, G. B., "The Motion of Two Spheres in a Viscous Fluid," Proc. Roy. Soc. London, A,111, 110 (1926).

33. Maude, A. D., "End Effects in a Falling-sphere Vixcometer," Brit. J. App. Physics, 12, 293 (1961).

34. Brenner, H., "The Slow Motion of a Sphere Through a Viscous Fluid Towards a Plane Surface," Chem. Eng. Sci., 16, 242 (1961).

35. Wakiya, S., Niigata Univ. (Nagooka Japan) Coll. Eng. Res. Report, No. 6, March 30 (1957).

36. Davis, M. H. and Sartor, J. D., "Theoretical Collision Efficiencies for Small Cloud Droplets in Stokes Flow," Nature, 215, 1371 (1967).

37. O'Neill, M. E., "Slow Motion of Viscous Liquid Caused by a Slowly Moving Solid Sphere," Mathematika, 11, 67 (1964).

38. Dean, W. R. and O'Neill, M. E., "A Slow Motion of Viscous Liquid Caused by the Rotation of a Solid Sphere," Mathematika, 10, 13 (1963).

39. Wakiya, S., "Slow Motions of a Viscous Fluid Around Two Spheres," J. Phys. Soc. Japan, 22, 1101 (1967).

40. Davis, M. H., "The Slow Translation and Rotation of Two Unequal Spheres in a Viscous Fluid," Chemical Engineering Science, 24, 1769 (1969).

41. Happel, J. and Brenner, H., Low Reynolds Number Hydrodynamics, Englewood Cliffs, New Jersey, Prentice-Hall, 516 (1965).

42. Goldman, A. J., Cox, R. G., and Brenner, H., "The Slow Motion of Two Identical Arbitrarily Oriented Spheres Through a Viscous Fluid," Chem. Eng. Sci., 21, 1151 (1966).

43. Eveson, G. F., Hall, E. W., and Ward, S. G., "Interaction Between Two Equal-Sized Equal-Settling Spheres Moving Through a Viscous Liquid," British J. of Applied Physics, 10, 43 (1959).

44. Mathews, H. W., and Smith, F. B., Br. J. of Appl. Phys., 11, 87 (1960).

45. Slack, G. W., and Mathews, H. W., "The Mutual Interaction Between Sedimenting Particles, Part I. The Sedimentations of Compact Clusters of Spheres in a Viscous Medium," Chemical Defense Experimental Establishment, Porton, Nr. Salisbury (1961).

46. Jayawiera, K. O. L. F., Mason, B. J., and Slack, G. W., J Fluid Mech., 20, 121 (1964).

47. Klett, J. D., "The Interaction and Motion of Rigid Spheres Falling in a Viscous Fluid at Low Reynolds Numbers," Ph.D. Dissertation, U.C.L.A. (1968) Unpublished.

48. Landeau, L. D. and Lifshitz, E. M., Fluid Dynamics, Pergamon Press (1959).

49. Bird, R. B., Stewart, W. E., and Lightfoot, E. N., Transport Phenomena, New York, Wiley (1960).

50. Brock, J. R., "On the Theory of Thermal Forces Acting on Aerosol Particles," Journal of Colloid Science, 17, 768-780 (1962).

51. Brock, J. R., "Investigation of a First-Order Slip-Flow Continuum Analysis: The Thermal Force," Journal of Physical Chemistry, 66, 1763 (1962).

52. Berker, R. in Encyclopedia of Physics: Fluid Dynamics II Vol VIII/2, p. 247. Springer-Verlog, Berlin (1963).

53. Brenner, H., "The Stokes Resistance of an Arbitrary Particle - II An Extension," Chem. Eng. Sci., 19, 599 (1964).

54. Carstens, J. C. and Kassner, J. L. Jr., "Some Aspects of Droplet Growth Theory Applicable to Nuclei Measurements" J. Rech. Atmos., 3, 33 (1968).

55. Morse, P. M. and Feshbach, H., Methods of Theoritical Physics, McGraw-Hill, New York, 1298 (1953).

56. Carstens, J. C., Williams, A., and Zung, J., "Theory of Droplet Growth in Clouds: II Diffusional Interaction Between Two Growing Droplets," J. Atmos. Sci., 27, 798 (1970).

57. Williams, A. L., and Carstens, J. C., "A Note Concerning the Interaction of Two Growing Water Droplets." J. Atmos. Sci., 28, 1298 (1971).

58. Rainville, E. D., Special Functions, The Macmillan Company, New York (1960).

59. Rosinski, J., "A Possible Role of Ice Forming Nuclei in Rain Formation" J of Applied Meteor., 6, 1062 (1967).

60. Abraham, Farid F., "A Physical Interpretation of the Structure of the Ventilation coefficients for Freely Falling Waterdrops" Journal of Atmos. Sci., 25, 76 (1968).

61. Fleagle, R. G. and J. A. Businger, An Introduction to Atmospheric Physics, Academic Press, New York and London (1963).

VITA

The author was born August 19, 1947, in Effingham, Illinois. He graduated from North Clay Community High School in 1965 and entered Eastern Illinois University, where he majored in physics and received a BS. in Ed. in August 1968. Since entering graduate school at the University of Missouri at Rolla, in September 1968, he has received the M.S. in Physics in May 1970 and has been a doctoral candidate in the Graduate Center for Cloud Physics Research, University of Missouri at Rolla.

The author is married to the former Miss Janice Sue Logsdon.

APPENDIX

A. Computer Program

The first 198 lines of the program are mainly devoted to reading in the necessary data and setting the position of the two spheres in bispherical coordinates. Solutions to the boundary condition equations specifying the unknown constants for determination of the temperature and vapor density profiles are given in lines 198-509. By altering the index IR this part of the program can be made to describe either a juxtaposition of two volatile particles or the situation in which one particle is volatile the other inert.

Lines 509 - 597 are devoted to calculating the diffusiophoretic force and a check on this calculation is done in lines 598 - 611.

The sum of the gravitational force on each particle parallel to the line joining centers and the diffusiophoretic force, as well as the component of the gravitational force perpendicular to the line of centers is found in lines 614 - 619.

With the forces known, the instantaneous velocities of each particle paralled to the line of centers (lines 620 - 700) and the corresponding velocities for motion perpendicular to the line of centers (lines 701 - 1046) are found.

The particles are allowed to fall an increment of time, DT, at these velocities resulting in a new orientation for which the process of calculating the diffusiophoretic force and the resulting instantaneous velocities is repeated. The time increment, DT, is adjusted (lines 1047 - 1064) at various points in the trajectory

according to specified tolerances to keep both the error in the trajectory and the computer time at reasonably small values. (The approximate computer time for one trajectory is about one hour.)

SUBROUTINE ALW - The program is treated as a subroutine and stored on a disc to avoid wasting compile time.

A1,A2 - Radii of spheres 1 and 2 respectively.

X10,X20 - Horizontal positions of spheres 1 and 2.

Z10,Z20 - Vertical positions of spheres 1 and 2.

BC1,BC2,CC1,CC2 - Constants defined in the thermal equilibrium boundary condition.

AD - Diffusion coefficient.

CNLAT1,CNLAT2 - Latent heats of spheres 1 and 2.

AKO - Thermal conductivity of saturated air.

AKI1,AKI2 - Internal thermal conductivities of spheres 1 and 2 respectively

TR,RHR - Bulk values of temperature and vapor density respectively.

SS1,SS2 - Supersaturation with respect to spheres 1 and 2 respectively.

GRAV - Acceleration of gravity.

V1X,V2X - Horizontal velocities of spheres 1 and 2 respectively.

V1Z,V2Z - Vertical velocities of spheres 1 and 2.

DA - Distance between sphere centers.

ALF - Defined as α in text (Table 4).

U10 = μ_1

U20 = μ_2

A(N,M),B(N) - Coefficient matrix and resultant vector to solve temperature and density profile boundary condition equations.

AA(N,M),BB(N) - Coefficient matrix and resultant vector to solve boundary condition equations for diffusiophoretic force.

DGELG - Tabulated subprogram for solving simultaneous equations.

F1,F2 - Diffusiophoretic force on particles 1 and 2 respectively.

FPL1,FPL2 - Force parallel to the line joining centers on particles 1 and 2 respectively.

FPD1,FPD2 - Force perpendicular to the line of centers on particles 1 and 2.

```
0001                DOUBLE PRECISION AP(122,122),BP(122)
0002              93 FORMAT(4I6)
                  C  IR=1 DENOTES INERT PARTICLE  IR=2--- VOLATILE PARTICLE
                  C   IN=1 ACTIVATES PROFILE CALC.  IN=2 DOES NOT
                  C  IP DENOTES DIMENSION OF PROFILE MATRIX
                  C   JF DENOTES DIMINSION OF PERPENDICULAR FORCE MATRIX
0003                READ(1,93)IP,JF,IR,IN
0004                CALL ALW(AP,BP,JF,IP,IR,IN)
0005                STOP
0006                END
0001                SUBROUTINE ALW(AP,BP,JF,IP,IR,IN)
                  C     ATMOSPHERIC CONDITIONS
0002                IMPLICIT REAL*8(A-H,O-Z)
0003                REAL*4 ETS
0004                DIMENSION AP(JF,JF),BP(JF),AN1(35),AN2(35),BN1(35),BN2(35)
0005                DIMENSION AB1(35),AB2(35),CD1(35),CD2(35),EF1(36),EF2(36),GH1(34)
                   1,GH2(34)
0006                DIMENSION ARAP(35),ARBP(35),ARAM(35),ARBM(35)
0007                DIMENSION X(300)
0008                DIMENSION PHE1(20),PHE2(20),PHI1(20),PHI2(20),GAP1(20),GAP2(20),
                   1H(20),E(20),C(20),D(20),AA(4,4),BB(4),A(96,96),B(96)
0009                DIMENSION SJ1(10),SJ2(10),SJ3(10),SJ4(10),DM1(10),DM2(10),DM3(10),
                   1DM4(10),RE1(10),RE2(10),RE3(10),RE4(10)
0010                DIMENSION ASP(10),BSP(10),CSP(10),DSP(10)
0011                DIMENSION AS(10),BS(10),CS(10),DS(10)
0012                DIMENSION X1W(5),W1X(5)
0013                DIMENSION VE1X(120),VE2X(120),VE1Z(120),VE2Z(120),FOR1(120),
                   1FOR2(120),DIST(120),ANGL(120)
0014                DIMENSION CHGX(120),CHGZ(120)
0015                DOUBLE PRECISION DSQRT,DLOG,DTANH,DEXP,DCOSH,DSINH,DABS
0016                DOUBLE PRECISION DATAN,DCOS,DSIN,DTAN
0017              1 FORMAT (4D18.8)
0018            100 FORMAT(3D18.8)
0019              2 FORMAT(//)
0020              3 FORMAT (6D16.6)
0021              5 FORMAT (E18.8,I6)
0022             11 FORMAT(' THE RESULTANT VECTOR -- B(N) ')
0023             12 FORMAT('  Z                        U                        T
                   1        RHO')
0024             13 FORMAT(' THE COFICIENTS OF TEMP + DENSITY ')
0025             14 FORMAT('        R1                R2                S1                S2
                   1                S1E               S2E    ')
0026             15 FORMAT(' THE COEFICIENT MATRIX IS -- A(N,J) ')
0027             16 FORMAT(T8,'A1',T24,'A2')
0028             17 FORMAT('              BC1                BC2                CC1
                   1           CC2 ')
```

```
0029          18 FORMAT('  ---     AD                  CNLAT1              CNLAT2
     1       AKO ')
0030          19 FORMAT('          AKI1                AKI2                TR
     1      RHR ')
0031          21 FORMAT('         GAME1               GAME2               GAMI1
     1 GAMI2              BP1                 BP2 ')
0032          22 FORMAT('          BP3                 BP4                 CP1
     1 CP2                TO1                 TO2 ')
0033          23 FORMAT(T6,'DA',T22,'U10',T38,'U20',T54,'AM',T70,'DA1',T86,'DA2')
0034          24 FORMAT('          Z1R                 Z1L                 Z2R
     1       Z2L  ')
0035          25 FORMAT('          ETS                  IER ')
0036          31 FORMAT('   Y1                  T1                  Y2
     1   T2  ')
0037          34 FORMAT('          VIS                 MG                  MV
     1SLP          ')
0038          37 FORMAT('        RHO1                RHO2        ')
0039          38 FORMAT('        PHE1                PHE2        ')
0040          39 FORMAT('        H(N)                E(N)                C(N)
     1       D(N)     ')
0041          40 FORMAT('-------------------------------------------------- ')
0042          41 FORMAT('          DA                  V1                  V2      ')

0043          42 FORMAT('         AS                  BS                  CS
     1      DS      ')
0044          44 FORMAT('         AA                 CC                  B1                  B2
     1                D1                  D2      ')
0045          45 FORMAT('        PHI1                PHI2                GAP1
     1      GAP2      ')
0046          46 FORMAT('         ASP                 BSP                 CSP
     1      DSP      ')
0047          47 FORMAT('         Y1P                 Y2P                 Y1PP                Y2PP
     1                VP                  VPP    ')
0048          52 FORMAT(T8,'F1',T24,'F2')
0049          53 FORMAT(T8,'SI1',T24,'SI2',T42,'DSI1',T60,'DSI2')
0050          54 FORMAT(T8,'V1',T24,'V2')
0051          55 FORMAT('  THE PERPENDICULAR VELOCTY COEFICIENTS ARE  ')
0052          56 FORMAT(' COLLISION ')
0053          57 FORMAT('  HIT ')
0054          58 FORMAT(' MISS')
0055          59 FORMAT(T8,'DA',T24,'ALF',T40,'EFF',T56,'A1A2')
0056          60 FORMAT(T8,'DA',T24,'ALF')
0057          61 FORMAT(T8,'X10',T24,'X20')
0058          62 FORMAT(' VALUES FROM LOOP 701 ')
0059          63 FORMAT('VALUES FROM LOOP 700 ')
0060          64 FORMAT(T8,'DA',T24,'ALF',T40,'EFF')
0061          65 FORMAT(T8,'DA',T24,'ALF',T40,'TT')
0062          66 FORMAT(' S AND J BOUNDARY CONDITION CHECK  ')
```

```
0063            67 FORMAT('  MAUDE BOUNDARY CONDITION CHECK ')
0064            68 FORMAT(T8,'SJ1',T24,'SJ2',T40,'SJ3',T56,'SJ4')
0065            69 FORMAT(T8,'RE1',T24,'RE2',T40,'RE3',T56,'RE4')
0066            70 FORMAT(T8,'DM1',T24,'DM2',T40,'DM3',T56,'DM4')
0067            71 FORMAT(T8,'FPD1',T24,'FPD2',T40,'FPD1P',T56,'FPD2P')
0068            72 FORMAT(T8,'CHK1',T24,'CHK2')
0069            73 FORMAT(T8,'A1',T24,'A2')
0070            76 FORMAT(T8,'AN1',T24,'BN1',T40,'AN2',T56,'BN2')
0071            77 FORMAT(5D17.7)
0072            78 FORMAT(I6)
0073            79 FORMAT(T8,'AB1',T24,'AB2',T40,'CD1',T50,'CD2')
0074            80 FORMAT(T8,'EF1',T24,'EF2')
0075            81 FORMAT(T8,'GH1',T24,'GH2')
0076            82 FORMAT(T8,'CND11',T24,'CND12')
0077            83 FORMAT(T8,'CND21',T24,'CND22')
0078            84 FORMAT(T8,'CND31',T24,'CND32')
0079            85 FORMAT(T8,'CND41',T24,'CND42')
0080            86 FORMAT(T8,'CND51',T24,'CND52')
0081            87 FORMAT(T8,'ARB1',T24,'ARB2',T39,'ARB3',T56,'BRB1',T74,'BR82',T89
                  1,'BRB3')
0082            88 FORMAT('  THE MATRIX ELEMENTS AFTER MULTIPLICATION ARE ---   ')
0083            89 FORMAT('    SUM   ')
0084            90 FORMAT(5D26.16)
0085            91 FORMAT('  CROSS OVER  ')
0086            93 FORMAT(4I6)
0087            94 FORMAT(4D26.16)
0088            95 FORMAT(T8,'X1',T24,'X2',T40,'Z1',T56,'Z2')
0089            96 FORMAT(T8,'V1X',T24,'V2X',T40,'V1Z',T56,'V2Z')
0090            97 FORMAT('   DT=DT/2   ')
0091            98 FORMAT('   DT=DT*2   ')
0092            99 FORMAT(T7,'DA',T23,'ALF',T39,'V1X',T55,'V1Z',T71,'V2X',T87,'V2Z')
0093            75 FORMAT(T8,'DA',T25,'F1',T42,'F2')
0094            32 FORMAT(T8,'SS1',T24,'SS2',T42,'RHR',T56,'SLP')

0095               WRITE(3,93)IP,JF,IR,IN
0096               READ(1,1)A1,A2
0097               READ(1,1)X10,X20,Z10,Z20
0098               READ(1,1) BC2,BC1,CC2,CC1
0099               READ(1,1) AD,CNLAT2,CNLAT1,AKO
0100               READ(1,1)SLP,PI,RHG,VIS
0101               READ(1,1)AKI2,AKI1,TR,SS2
0102               READ(1,1) TOLA,TOLR,DALF,GRAV
0103               READ(1,1)ERR1,ERR2,DT
0104               JE=1
0105               RHR=SS2*(BC2*TR+CC2)
0106               SS1=RHR/(BC1*TR+CC1)
0107               RHOI=.917
```

```
0108                WRITE(3,16)
0109                WRITE(3,1)A1,A2
0110                WRITE(3,2)
0111                WRITE(3,17)
0112                WRITE(3,1)BC1,BC2,CC1,CC2
0113                WRITE(3,2)
0114                WRITE(3,18)
0115                WRITE(3,1)AD,CNLAT1,CNLAT2,AKO
0116                WRITE(3,2)
0117                WRITE(3,19)
0118                WRITE(3,1)AKI1,AKI2,TR,RHR
0119                WRITE(3,2)
0120                SQ2=DSQRT(2.D0)
0121                GAMI1=AKI1/(AD*CNLAT1)
0122                GAMI2=AKI2/(AD*CNLAT2)
0123                GAME1=AKO/(AD*CNLAT1)
0124                GAME2=AKO/(AD*CNLAT2)
0125                BP1=BC1+GAME1
0126                BP2=BC2+GAME2
0127                BP3=BC2+GAME1
0128                BP4=BC1+GAME2
0129                TS=TR*SQ2
0130                CP1=SQ2*(CC1-RHR)
0131                CP2=SQ2*(CC2-RHR)
0132                TO1=(RHR-CC1+GAME1*TR)/BP1
0133                TO2=(RHR-CC2+GAME2*TR)/BP2
0134                WRITE(3,21)
0135                WRITE(3,3)GAME1,GAME2,GAMI1,GAMI2,BP1,BP2
0136                WRITE(3,2)
0137                WRITE(3,22)
0138                WRITE(3,3)BP3,BP4,CP1,CP2,TO1,TO2
0139                WRITE(3,2)
0140                WRITE(3,32)
0141                WRITE(3,1)SS1,SS2,RHR
0142                WRITE(3,2)
0143          801   X1=X10
0144                V1X=0
0145                V2X=0
0146                V1Z=0
0147                V2Z=0
0148                TT=0.
0149                INDP=1
0150                IND=0
0151                X2=X20
0152                Z1=Z10
```

```
0153              Z2=Z20
0154            606 CONTINUE
0155              DZ=Z1-Z2
0156              DX=X1-X2
0157              ARUG=DX*DX+DZ*DZ
0158              DA=DSQRT(ARUG)
0159              IF (DZ) 831,832,831
0160            832 ALF=PI/2.
0161              GO TO 835
0162            831 ALF=DATAN(DX/DZ)
0163            835 EFF=DX*DX/((A1+A2)**2)
0164              WRITE(3,62)
0165              WRITE(3,64)
0166              WRITE(3,1)DA,ALF,EFF
0167              TRACE=1.
0168              IF (EFF-.0005)825,825,800
0169            800 SAM=2*DA
0170              DIST(JE)=DA*10000.
0171              ANGL(JE)=ALF*57.29578
0172              DA1=(DA*DA+A1*A1-A2*A2)/SAM
0173              DA2=(DA*DA+A2*A2-A1*A1)/SAM
0174              AM=DSQRT((DA2+A2)*(DA2-A2))
0175              U10=DLOG((DA1+AM)/(DA1-AM))/2.D0
0176              U20=DLOG((DA2+AM)/(DA2-AM))/2.D0
0177              WRITE(3,73)
0178              WRITE(3,1)A1,A2
0179              WRITE(3,23)
0180              WRITE(3,3)DA,U10,U20,AM,DA1,DA2
0181              WRITE(3,2)
0182              F1=0.
0183              F2=0.
0184              IND=IND+1
0185              IF (IND-4)600,601,601
0186            601 W1X(1)=W1X(2)
0187              W1X(2)=W1X(3)
0188              X1W(1)=X1W(2)
0189              X1W(2)=X1W(3)
0190              IND=3
0191            600 CONTINUE
0192              X1W(IND)=X1
0193              V1XN=V1X
0194              V2XN=V2X
0195              V1ZN=V1Z
0196              V2ZN=V2Z
0197              IF (IN-1)699,699,799
0198            699 CONTINUE
              C     SOLUTION TO BOUNDARY CONDITION EQNS.
```

```
0199                I=IP
0200                I6=I/6
0201                I23=2*I/3
0202                I3=I/3
0203                I2=I/2
0204                I3P=I3+1
0205                I2P=I2+1
0206                I23P=I23+1
0207                I56=5*I/6
0208                I56M=I56-1
0209                IM2=I-2
0210                I23M=I23-1
0211                I2M=I2-1
0212                I6M=I6-1
0213                I6MM=I6M-1
0214                I6P=I6+1
0215                I3M=I3-1
0216                I56P=I56+1
0217                DO 700 N=1,I
0218                DO 700 J=1,I
0219           700  A(N,J)=0.0
0220                DO 701 N=1,I23
0221                J=N
0222           701  A(N,J)=1.0
0223                DO 702 N=1,I6
0224                J=N+I6
0225                K=N-1
0226                CK=K
0227                U1K=(2.*CK+1.)*U10
0228           702  A(N,J)=DEXP(U1K)
0229                DO 703 N=1,I3
0230                J=N+I23
0231           703  A(N,J)=-1.0
0232                DO 704 J=1,I6
0233                N=J+I6
0234                K=J-1
0235                CK=K
0236                U2K=(2.*CK+1.)*U20
0237           704  A(N,J)=DEXP(U2K)
0238                DO 705 N=I3P,I2
0239                J=N+I6
0240                K=N-I3P
0241                CK=K
0242                U1K=(2.*CK+1.)*U10
0243           705  A(N,J)=DEXP(U1K)
0244                DO 706 N=I3P,I2
```

```
0245              J=N+I3
0246          706 A(N,J)=-BC1
0247              DO 707 N=I2P,I23
0248              J=N+I3
0249          707 A(N,J)=-BC2
0250              DO 708 N=I2P,I23
0251              J=N-I6
0252              K=N-I2P
0253              CK=K
0254              U2K=(2.*CK+1.)*U20
0255          708 A(N,J)=DEXP(U2K)
0256              JM=1
0257              DO 709 N=I23P,I56M
0258              J=N-I23
0259              JP=J+1
0260              K=N-I23P
0261              L=K+1
0262              M=K-1
0263              CK=K
0264              CL=L
0265              CM=M
0266              U1K=(CK+.5)*U10
0267              U1M=(CM+.5)*U10
0268              U1L=(CL+.5)*U10
0269              T11=DSINH(U10)-(2.*CK+1.)*DCOSH(U10)
0270              A(N,JM)=CK*GAME1*DEXP(-U1M)
0271              A(N,J)=GAME1*T11*DEXP(-U1K)
0272              A(N,JP)=CL*GAME1*DEXP(-U1L)
0273          709 JM=J
0274              DO 710 N=I23P,I56M
0275              J=N-I2
0276              JM=J-1
0277              JP=J+1
0278              K=N-I23P
0279              L=K+1
0280              M=K-1
0281              CL=L
0282              CK=K
0283              CM=M
0284              U1K=(CK+.5)*U10
0285              U1M=(CM+.5)*U10
0286              U1L=(CL+.5)*U10
0287               T12=DSINH(U10)+(2.*CK+1.)*DCOSH(U10)
0288              A(N,J)=GAME1*T12*DEXP(U1K)
0289              A(N,JM)=-GAME1*CK*DEXP(U1M)
0290          710 A(N,JP)=-GAME1*CL*DEXP(U1L)
0291              DO 711 N=I23P,I56M
```

```
0292                J=N-I3
0293                JM=J-1
0294                JP=J+1
0295                K=N-I23P
0296                L=K+1
0297                M=K-1
0298                CL=L
0299                CK=K
0300                CM=M
0301                U1K=(CK+.5)*U10
0302                U1M=(CM+.5)*U10
0303                U1L=(CL+.5)*U10
0304                T11=DSINH(U10)-(2.*CK+1.)*DCOSH(U10)
0305                A(N,J)=T11*DEXP(-U1K)
0306                A(N,JM)=CK*DEXP(-U1M)
0307          711   A(N,JP)=CL*DEXP(-U1L)
0308                DO 712 N=I23P,I56M
0309                J=N-I6
0310                JM=J-1
0311                JP=J+1
0312                K=N-I23P
0313                L=K+1
0314                M=K-1
0315                CL=L
0316                CM=M
0317                CK=K
0318                U1K=(CK+.5)*U10
0319                U1M=(CM+.5)*U10
0320                U1L=(CL+.5)*U10
0321                 T12=DSINH(U10)+(2.*CK+1.)*DCOSH(U10)
0322                A(N,J)=T12*DEXP(U1K)
0323                A(N,JM)=-CK*DEXP(U1M)
0324          712   A(N,JP)=-CL*DEXP(U1L)
0325                DO 713 N=I23P,I56M
0326                 J=N
0327                 JM=J-1
0328                 JP=J+1
0329                 K=N-I23P
0330                 L=K+1
0331                 M=K-1
0332                 CK=K
0333                 CM=M
0334                 CL=L
0335                 U1K=(CK+.5)*U10
0336                 U1M=(CM+.5)*U10
0337                 U1L=(CL+.5)*U10
0338                 T11=DSINH(U10)-(2.*CK+1.)*DCOSH(U10)
```

```
0339              A(N,J)=-GAMI1*T11*DEXP(-U1K)
0340              A(N,JM)=-GAMI1*CK*DEXP(-U1M)
0341          713 A(N,JP)=-GAMI1*CL*DEXP(-U1L)
0342              JM=1
0343              DO 714 N=I56,IM2
0344              J=N-I56M
0345              JP=J+1
0346              K=N-I56
0347              L=K+1
0348              M=K-1
0349              CL=L
0350              CK=K
0351              CM=M
0352              U2L=(CL+.5)*U20
0353              U2K= (CK+.5)*U20
0354              U2M=(CM+.5)*U20
0355              T21=-DSINH(U20)-(2.*CK+1.)*DCOSH(U20)
0356              A(N,JM)=CK*GAME2*DEXP(U2M)
0357              A(N,J)=GAME2*T21*DEXP(U2K)
0358              A(N,JP)=CL*GAME2*DEXP(U2L)
0359          714 JM=J
0360              DO 715 N=I56,IM2
0361              J=N-I23M
0362              JM=J-1
0363              JP=J+1
0364              K=N-I56
0365              L=K+1
0366              M=K-1
0367              CK=K
0368              CL=L
0369              CM=M
0370              U2L=(CL+.5)*U20
0371              U2K= (CK+.5)*U20
0372              U2M=(CM+.5)*U20
0373              T22=-DSINH(U20)+(2.*CK+1.)*DCOSH(U20)
0374              A(N,J)=+GAME2*T22*DEXP(-U2K)
0375              A(N,JM)=-CK*GAME2*DEXP(-U2M)
0376          715 A(N,JP)=-CL*GAME2*DEXP(-U2L)
0377              DO 718 N=I56,IM2
0378              J=N+1
0379              JM=J-1
0380              JP=J+1
0381              K=N-I56
0382              L=K+1
0383              M=K-1
```

```
0384                CL=L
0385                CM=M
0386                CK=K
0387                U2L=(CL+.5)*U20
0388                U2K= (CK+.5)*U20
0389                U2M=(CM+.5)*U20
0390                T22=-DSINH(U20)+(2.*CK+1.)*DCOSH(U20)
0391                A(N,J)=-GAMI2*T22*DEXP(-U2K)
0392                A(N,JM)=GAMI2*CK*DEXP(-U2M)
0393          718   A(N,JP)=GAMI2*CL*DEXP(-U2L)
0394                N=I-1
0395                DO 719 J=I6P,I3
0396                K=J+I3
0397                A(N,J)=GAME1
0398          719   A(N,K)=1.0
0399                N=I
0400                DO 720 J=1,I6
0401                K=J+I3
0402                A(N,J)=GAME2
0403          720   A(N,K)=1.
0404                DO 722 J=I3P,I2
0405                K=J+I6
0406                B(J)=CP1
0407          722   B(K)=CP2
0408                DO 721 J=1,I3
0409                K=J+I23
0410                B(J)=-TS
0411          721   B(K)=0.0
0412                IF (IR-1)7000,7000,7001
0413           7001 CONTINUE
               C     VOLATILE BOUNDARY CONDITION
0414                DO 7725 J=1,I6
0415                K=J+I6
0416                B(J)=-TS
0417           7725 B(K)=-TS
0418                DO 7716 N=I56,IM2
0419                J=N-I2M
0420                K=N-I56
0421                JM=J-1
0422                JP=J+1
0423                L=K+1
0424                M=K-1
0425                CL=L
0426                CK=K
0427                CM=M
0428                U2L=(CL+.5)*U20
0429                U2K= (CK+.5)*U20
```

```
0430                U2M=(CM+.5)*U20
0431                T21=-DSINH(U20)-(2.*CK+1.)*DCOSH(U20)
0432                A(N,J)=T21*DEXP(U2K)
0433                A(N,JM)=CK*DEXP(U2M)
0434          7716   A(N,JP)=CL*DEXP(U2L)
0435                DO 7717 N=I56,IM2
0436                J=N-I3M
0437                K=N-I56
0438                JM=J-1
0439                JP=J+1
0440                L=K+1
0441                M=K-1
0442                CL=L
0443                CM=M
0444                CK=K
0445                U2L=(CL+.5)*U20
0446                U2K= (CK+.5)*U20
0447                U2M=(CM+.5)*U20
0448                T22=-DSINH(U20)+(2.*CK+1.)*DCOSH(U20)
0449                A(N,J)=T22*DEXP(-U2K)
0450                A(N,JM)=-CK*DEXP(-U2M)
0451          7717  A(N,JP)=-CL*DEXP(-U2L)
0452                GO TO 7002
0453          7000  CONTINUE
              C     INERT BOUNDARY CONDITION
0454                DO 716 N=I2P,I23M
0455                J=N-I6
0456                K=N-I2P
0457                JM=J-1
0458                JP=J+1
0459                L=K+1
0460                M=K-1
0461                CL=L
0462                CK=K
0463                CM=M
0464                U2L=(CL+.5)*U20
0465                U2K= (CK+.5)*U20
0466                U2M=(CM+.5)*U20
0467                T21=-DSINH(U20)-(2.*CK+1.)*DCOSH(U20)
0468                A(N,J)=T21*DEXP(U2K)
0469                A(N,JM)=CK*DEXP(U2M)
0470           716   A(N,JP)=CL*DEXP(U2L)
0471                DO 717 N=I2P,I23M
0472                J=N
0473                JM=J-1
0474                JP=J+1
0475                K=N-I2P
```

```
0476                L=K+I
0477                M=K-1
0478                CL=L
0479                CM=M
0480                CK=K
0481                U2L=(CL+.5)*U20
0482                U2K= (CK+.5)*U20
0483                U2M=(CM+.5)*U20
0484                T22=-DSINH(U20)+(2.*CK+1.)*DCOSH(U20)
0485                A(N,J)=T22*DEXP(-U2K)
0486                A(N,JM)=-CK*DEXP(-U2M)
0487          717   A(N,JP)=-CL*DEXP(-U2L)
0488                A(I23,I23)=0
0489                DO 723 J=I3P,I2
0490                N=I23
0491          723   A(N,J)=1.
0492                DO 724 N=I2P,I23
0493                J=N+I3
0494                A(N,J)=0.
0495          724   B(N)=0.
0496                DO 725 J=1,I6
0497                N=I
0498                K=J+I3
0499                A(N,J)=0.0
0500          725   A(N,J)=1.
0501         7002   CONTINUE
0502                ETS=.1E-16
0503                CALL DGELG(B,A,I,1,ETS,IER)
0504                WRITE(3,13)
0505                WRITE(3,1)(B(N),N=1,I)
0506                WRITE(3,2)
0507                WRITE(3,25)
0508                WRITE(3,5)ETS,IER
0509                WRITE(3,2)
              C   CALCULATION OF PHORETIC FORCE
0510                RHO1=0.
0511                RHO2=0.
0512                DO 403 N=1,10
0513                CN=N-1
0514                NC=I3+N
0515                ND=I2+N
0516                XN=CN+.5
0517                UN1=XN*U10
0518                UN2=XN*U20
0519                PHE1(N)=B(NC)*DEXP(-UN1)+B(ND)*DEXP(UN1)
0520                PHE2(N)=B(NC)*DEXP(UN2)+B(ND)*DEXP(-UN2)
0521                RHO1=RHO1+PHE1(N)
0522          403   RHO2=RHO2+PHE2(N)
```

```
0523                RHO1=DSQRT(DCOSH(U10)-1.)*RHO1+RHR
0524                RHO2=DSQRT(DCOSH(U20)-1.)*RHO2+RHR
0525                WRITE(3,37)
0526                WRITE(3,1)RHO1,RHO2
0527                WRITE(3,2)
0528                DO 401 N=1,7
0529                CN=N
0530                NC=I3+N
0531                ND=I2+N
0532                XN=CN+.5
0533                XM=CN-.5
0534                XK=CN+1.5
0535                TXM=2.*XM
0536                TXN=2.*XN
0537                TXK=2.*XK
0538                UN1=XN*U10
0539                UN2=XN*U20
0540                UM1=XM*U10
0541                UM2=XM*U20
0542                UK1=XK*U10
0543                UK2=XK*U20
0544                NP=N+2
0545                NPP=N+1
0546                PHI1(N)=PHE1(N)+PHE1(NP)-2.*DCOSH(U10)*PHE1(NPP)
0547                PHI2(N)=PHE2(N)+PHE2(NP)-DCOSH(U20)*PHE2(NPP)*2.
0548                SIM=DSINH(UM1+UM2)
0549                GAP1(N)=+(1.-SLP)*AD*(AM/RHG)*PHI1(N)*N*(N+1)*DCOSH(UM1)*SIM/TXN
0550                GAP2(N)=GAP1(N)*PHI2(N)*DCOSH(UM2)/DCOSH(UM1)/PHI1(N)
0551                GAP1(N)=GAP1(N)/(DCOSH(UM1)*SIM)
0552                GAP2(N)=GAP2(N)/(DCOSH(UM2)*SIM)
0553                AA(1,1)=DCOSH(UM1)
0554                AA(1,2)=DSINH(UM1)
0555                AA(1,3)=DCOSH(UK1)
0556                AA(1,4)=DSINH(UK1)
0557                AA(3,1)=DCOSH(UM2)
0558                AA(3,2)=-DSINH(UM2)
0559                AA(3,3)=DCOSH(UK2)
0560                AA(3,4)=-DSINH(UK2)
0561                AA(2,1)=TXM*DSINH(UM1)
0562                AA(2,2)=TXM*DCOSH(UM1)
0563                AA(2,3)=TXK*DSINH(UK1)
0564                AA(2,4)=TXK*DCOSH(UK1)
0565                AA(4,1)=-TXM*DSINH(UM2)
0566                AA(4,2)=TXM*DCOSH(UM2)
0567                AA(4,3)=-TXK*DSINH(UK2)
0568                AA(4,4)=TXK*DCOSH(UK2)
```

```
0569                BB(1)=0.
0570                BB(3)=0.
0571                BB(2)=GAP1(N)
0572                BB(4)=GAP2(N)
0573                CALL DGELG(BB,AA,4,1,ETS,IER)
0574                WRITE(3,25)
0575                WRITE(3,1)ETS,IER
0576                H(N) = BB(1)
0577                E(N) = BB(2)
0578                C(N) = BB(3)
0579                D(N) = BB(4)
0580                F1=-TXN*(H(N)+E(N)+C(N)+D(N))+F1
0581           401  F2=TXN*(H(N)-E(N)+C(N)-D(N))+F2
0582                WRITE(3,2)
0583                COF=-VIS*3.1416*2.*SQ2/AM
0584                F1=COF*F1
0585                F2=COF*F2
0586                WRITE(3,39)
0587                WRITE(3,1)(H(N),E(N),C(N),D(N),N=1,7)
0588                WRITE(3,2)
0589                WRITE(3,52)
0590                WRITE(3,1)F1,F2
0591                FOR2(JE)=F2*.1000D+09
0592                FOR1(JE)=F1*.1000D+09
0593                V1=F1*10000./(6.*PI*VIS*A1)
0594                 V2=F2*10000./(6.*PI*VIS*A2)
0595                WRITE(3,54)
0596                WRITE(3,1)V1,V2
0597                WRITE(3,2)
                C       BOUNDARY CONDITION CHECK
0598                DO 666 N=1,7
0599                CN=N
0600                UM1=(CN-.5)*U10
0601                UM2=(CN-.5)*U20
0602                UK1=(CN+1.5)*U10
0603                UK2=(CN+1.5)*U20
0604                SI1=H(N)*DCOSH(UM1)+E(N)*DSINH(UM1)+C(N)*DCOSH(UK1)+D(N)
                   1*DSINH(UK1)
0605                SI2=H(N)*DCOSH(UM2)-E(N)*DSINH(UM2)+C(N)*DCOSH(UK2)-D(N)
                   1*DSINH(UK2)
0606                SIM=DSINH(UM1+UM2)
0607                DSI1=(2.*CN-1.)*(H(N)*DSINH(UM1)+E(N)*DCOSH(UM1))+(2.*CN+3.)*
                   1(C(N)*DSINH(UK1)+D(N)*DCOSH(UK1))-GAP1(N)
0608                DSI2=(2.*CN-1.)*(-H(N)*DSINH(UM2)+E(N)*DCOSH(UM2))+(2.*CN+3.)
```

```
     1*(-C(N)*DSINH(UK2)+D(N)*DCOSH(UK2))-GAP2(N)
0609       WRITE(3,53)
0610       WRITE(3,1)SI1,SI2,DSI1,DSI2
0611       WRITE(3,2)
0612   666 CONTINUE
0613   799 CONTINUE
0614       FG1=-4./3.*PI*A1*A1*A1*GRAV
0615       FG2=-4./3.*PI*A2*A2*A2*GRAV
0616       FPL2=FG2*DCOS(ALF)+F2
0617       FPL1=FG1*DCOS(ALF)+F1
0618       FPD1=FG1*DSIN(ALF)
0619       FPD2=FG2*DSIN(ALF)
C    CALCULATION OF STOKES RESISTANCE
0620       COF=-VIS*3.1416*2.*SQ2/AM
0621       S1=6.*3.1416*VIS*A1
0622       S2=S1*A2/A1
0623       R1=FPL1/S1
0624       R2=FPL2/S2
0625       COF1=COF/S1
0626       COF2=COF/S2
0627       Y1P=0.
0628       Y2P=0.
0629       Y1PP=0.
0630       Y2PP=0.
0631       DO 402 N=1,10
0632       XM=N-.5
0633       XK=N+1.5
0634       TXM=2.*XM
0635       TXK=2.*XK
0636       XP=N+.5
0637       TXP=2.*XP
0638       UM1=XM*U10
0639       UM2=XM*U20
0640       UK1=XK*U10
0641       UK2=XK*U20
0642       UP1=XP*U10
0643       UP2=XP*U20
0644       DELT=4.*DSINH(UP1+UP2)*DSINH(UP1+UP2)-TXP*TXP*DSINH(U10+U20)
     1*DSINH(U10+U20)
0645       DEL=1./DELT
```

```
0646                GK=AM*AM*N*(N+1)/(SQ2*TXM*TXP*TXK)
0647                AS(N)=DEL*GK*TXK*(4.*DEXP(-UP1-UP2)*DSINH(UP1+UP2)+TXP*TXP*
                   1DEXP(U10+U20)*DSINH(U10+U20)+2.*TXM*DSINH(UP1+UP2)*DCOSH(UP1-UP2)
                   2-2.*TXP*DSINH(UK1+UK2)*DCOSH(UM1-UM2)-TXP*TXM*DSINH(U10+U20)*
                   3DCOSH(U10-U20))
0648                BS(N)=-DEL*TXK*GK*(2.*TXM*DSINH(UP1+UP2)*DSINH(UP1-UP2)-2.*TXP*
                   1DSINH(UK1+UK2)*DSINH(UM1-UM2)+TXP*TXM*DSINH(U10+U20)
                   2*DSINH(U10-U20))
0649                CS(N)=-DEL*TXM*GK*(4.*DEXP(-UP1-UP2)*DSINH(UP1+UP2)-TXP*TXP
                   1*DEXP(-U10-U20)*DSINH(U10+U20)+2.*TXP*DSINH(UM1+UM2)
                   1*DCOSH(UK1-UK2)-2.*TXK*DSINH(UP1+UP2)*DCOSH(UP1-UP2)+TXP*TXK*
                   2DSINH(U10+U20)*DCOSH(U10-U20))
0650                DS(N)=DEL*TXM*GK*(2.*TXP*DSINH(UM1+UM2)*DSINH(UK1-UK2)-2.*TXK
                   1*DSINH(UP1+UP2)*DSINH(UP1-UP2)+TXP*TXK*DSINH(U10+U20)
                   2*DSINH(U10-U20))
0651                ASP(N)=TXK*GK*(2.*TXM*DSINH(UP1+UP2)*DSINH(UP1-UP2)-2.*TXP*
                   1DSINH(UK1+UK2)*DSINH(UM1-UM2)-TXM*TXP*DSINH(U10+U20)*
                   2DSINH(U10-U20))*DEL
0652                BSP(N)=-TXK*GK*(-4.*DEXP(-UP1-UP2)*DSINH(UP1+UP2)-TXP*TXP*
                   1DEXP(U10+U20)*DSINH(U10+U20)+2.*TXM*DSINH(UP1+UP2)*DCOSH(UP1-UP2)
                   2-2.*TXP*DSINH(UK1+UK2)*DCOSH(UM1-UM2)+TXM*TXP*DSINH(U10+U20)
                   3*DCOSH(U10-U20))*DEL
                C   CSP IS ARTIFICALLY SUPRESSED TO ZERO
0653                CSP(N)=-TXM*GK*(2.*TXP*DSINH(UM1+UM2)*DSINH(UK1-UK2)-2.*TXK
                   1*DSINH(UP1+UP2)*DSINH(UP1-UP2)-TXP*TXK*DSINH(U10+U20)*
                   2DSINH(U10-U20))*DEL
0654                DSP(N)=TXM*GK*(-4.*DEXP(-UP1-UP2)*DSINH(UP1+UP2)+TXP*TXP*
                   1DEXP(-U10-U20)*DSINH(U10+U20)+2.*TXP*DSINH(UM1+UM2)*DCOSH(UK1-UK2)
                   2-2.*TXK*DSINH(UP1+UP2)*DCOSH(UP1-UP2)-TXP*TXK*DSINH(U10+U20)
                   3*DCOSH(U10-U20))*DEL
0655                SJ1(N)=AS(N)*DCOSH(UM1)+BS(N)*DSINH(UM1)+CS(N)*DCOSH(UK1)
                   1+DS(N)*DSINH(UK1)
0656                SJ2(N)=AS(N)*DCOSH(UM2)-BS(N)*DSINH(UM2)+CS(N)*DCOSH(UK2)
                   1-DS(N)*DSINH(UK2)
0657                SJ3(N)=TXM*(AS(N)*DSINH(UM1)+BS(N)*DCOSH(UM1))+TXK*(CS(N)*
                   1DSINH(UK1)+DS(N)*DCOSH(UK1))
0658                SJ4(N)=TXM*(-AS(N)*DSINH(UM2)+BS(N)*DCOSH(UM2))+TXK*(-CS(N)*
                   1DSINH(UK2)+DS(N)*DCOSH(UK2))
0659                DM1(N)=ASP(N)*DCOSH(UM1)+BSP(N)*DSINH(UM1)+CSP(N)*DCOSH(UK1)+
                   1DSP(N)*DSINH(UK1)
```

```
0660            DM2(N)=ASP(N)*DCOSH(UM2)-BSP(N)*DSINH(UM2)+CSP(N)*DCOSH(UK2)-
               1DSP(N)*DSINH(UK2)
0661            DM3(N)=TXM*(ASP(N)*DSINH(UM1)+BSP(N)*DCOSH(UM1))+TXK*(CSP(N)*
               1DSINH(UK1)+DSP(N)*DCOSH(UK1))
0662            DM4(N)=TXM*(-ASP(N)*DSINH(UM2)+BSP(N)*DCOSH(UM2))+TXK*(-CSP(N)*
               1DSINH(UK2)+DSP(N)*DCOSH(UK2))
0663            RE1(N)=GK*(TXK*DEXP(-UM1)-TXM*DEXP(-UK1))
0664            RE2(N)=GK*(TXK*DEXP(-UM2)-TXM*DEXP(-UK2))
0665            RE3(N)=-GK*TXK*TXM*(DEXP(-UM1)-DEXP(-UK1))
0666            RE4(N)=GK*TXK*TXM*(DEXP(-UM2)-DEXP(-UK2))
0667            Y1P=COF1*TXP*(AS(N)+BS(N)+CS(N)+DS(N))+Y1P
0668            Y2P=Y2P+COF2*TXP*(AS(N)-BS(N)+CS(N)-DS(N))
0669            Y1PP=Y1PP+COF1*TXP*(ASP(N)+BSP(N)+CSP(N)+DSP(N))
0670      402   Y2PP=Y2PP+COF2*TXP*(ASP(N)-BSP(N)+CSP(N)-DSP(N))
0671            DUN=Y1PP*Y2P-Y2PP*Y1P
0672            VP=(R2*Y1PP-R1*Y2PP)/DUN
0673            VPP=(+R1*Y2P-R2*Y1P)/DUN
0674            V1PL=VP-VPP
0675            V2PL=VP+VPP
0676            WRITE(3,47)
0677            WRITE(3,3)Y1P,Y2P,Y1PP,Y2PP,VP,VPP
0678            WRITE(3,2)
0679            WRITE(3,42)
0680            WRITE(3,1)(AS(N),BS(N),CS(N),DS(N),N=1,10)
0681            WRITE(3,2)
0682            WRITE(3,46)
0683            WRITE(3,1)(ASP(N),BSP(N),CSP(N),DSP(N),N=1,10)
0684            WRITE(3,41)
0685            YAMB=R1/V1PL
0686            WRITE(3,1)DA,V1PL,V2PL,YAMB
0687            WRITE(3,2)
0688            DO 992 N=1,10
0689            BSJ1=SJ1(N)+RE1(N)
0690            BSJ2=SJ2(N)+RE2(N)
0691            BSJ3=SJ3(N)+RE3(N)
0692            BSJ4=SJ4(N)+RE4(N)
```

```
0693                BDM1=DM1(N)-RE1(N)
0694                BDM2=DM2(N)+RE2(N)
0695                BDM3=DM3(N)-RE3(N)
0696                BDM4=DM4(N)+RE4(N)
0697                WRITE(3,66)
0698                WRITE(3,1)BSJ1,BSJ2,BSJ3,BSJ4
0699                WRITE(3,67)
0700              992 WRITE(3,1)BDM1,BDM2,BDM3,BDM4
                C  MOTION PERPENDICULAR TO LINE OF CENTERS
0701                L=JF-2
0702                L8=L/8
0703                L4=L/4
0704                L2=L/2
0705                L23=2*L/3
0706                L56=5*L/6
0707                L512=5*L/12
0708                L58=5*L/8
0709                L78=7*L/8
0710                L34=3*L/4
0711                L38=3*L/8
0712                L712=7*L/12
0713                L1112=11*L/12
0714                LP=L+1
0715                LL=L+2
0716                L8M=L8-1
0717                L2P=L2+1
0718                L8P=L8+1
0719                L4P=L4+1
0720                L512P=L512+1
0721                L58P=L58+1
0722                FPD1P=FPD1/(6*PI*VIS*A1)
0723                FPD2P=FPD2/(6*PI*VIS*A2)
0724                DO 299 NR=1,LL
0725                DO 299 NC=1,LL
0726                AP(NR,NC)=0.
0727              299 BP(NR)=0.
0728                DO 298 N=1,L4
0729                UN1=(N-.5)*U10
0730                UN2=(N-.5)*U20
0731                AN1(N)=DEXP(UN1)/DSINH(U10)
0732                AN2(N)=-DEXP(-UN2)/DSINH(U20)
0733                BN1(N)=DEXP(-UN1)/DSINH(U10)
0734              298 BN2(N)=-DEXP(UN2)/DSINH(U20)
```

```
0735                NCM=3
0736                NRM=3
0737                DO 300 NR=1,L8
0738                NC=NR+L8
0739                NRP=NR+1
0740                NRQ=NRP+1
0741                AP(NR,NR)=-2.*DCOSH(U10)*AN1(NRP)
0742                AP(NR,NC)=-2.*DCOSH(U10)*BN1(NRP)
0743                AP(NC,NC)=-2.*DCOSH(U20)*BN2(NRP)
0744                AP(NC,NR)=-2.*DCOSH(U20)*AN2(NRP)
0745                COD=2.*(NR-1)/(2*NR-1.)
0746                AP(NR,NRM)=COD*AN1(NR)
0747                AP(NR,NCM)=COD*BN1(NR)
0748                AP(NC,NRM)=COD*AN2(NR)
0749                AP(NC,NCM)=COD*BN2(NR)
0750                NCM=NC
0751                NRM=NR
0752                NCP=NC+1
0753                CODE=2.*(NR+2)/(2*NR+3.)
0754                AP(NR,NRP)=CODE*AN1(NRQ)
0755                AP(NR,NCP)=CODE*BN1(NRQ)
0756                AP(NC,NRP)=CODE*AN2(NRQ)
0757                AP(NC,NCP)=CODE*BN2(NRQ)
0758                NCC=NC+L8
0759                NCD=NC+L4
0760                UN1=(NR+.5)*U10
0761                UN2=(NR+.5)*U20
0762                AP(NR,NCC)=-DEXP(UN1)
0763                AP(NR,NCD)=-DEXP(-UN1)
0764                AP(NC,NCC)=-DEXP(-UN2)
0765          300   AP(NC,NCD)=-DEXP(UN2)
0766                WRITE(3,2)
0767                DO 301 NR=1,L8P
0768                UN1=(NR-.5)*U10
0769                UN2=(NR-.5)*U20
0770                NC=NR+L8
0771                NRE=NR+L4
0772                NCE=NR+L2
0773                NCF=NR+L2+L8P
0774                AP(NRE,NCE)=-DEXP(UN1)
0775                AP(NRE,NCF)=-DEXP(-UN1)
0776                NP=NR+1
0777                NR1=L4+NR
0778                NREE=NR1+L8P
0779                AP(NREE,NCE)=-DEXP(-UN2)
0780                AP(NREE,NCF)=-DEXP(UN2)
0781                CAD=NR*(NR+1.)/(2*NR+1.)
```

```
0782                AP(NR1,NR)=CAD*AN1(NP)
0783                AP(NR1,NC)=CAD*BN1(NP)
0784                NR2=NR1+L8P
0785                AP(NR2,NR)=CAD*AN2(NP)
0786                AP(NR2,NC)=CAD*BN2(NP)
0787                AP(NR1,LP)=2.*SQ2*DEXP(-UN1)
0788          301   AP(NR2,LL)=2.*SQ2*DEXP(-UN2)
0789                DO 302 NR=2,L8
0790                UN1=(NR+.5)*U10
0791                UN2=(NR+.5)*U20
0792                NR1=L4P+NR
0793                NC=NR-1
0794                NC1=NC+L8
0795                NR2=NR1+L8P
0796                NRP=NR+1
0797                NCP=NRP+L8
0798                CAD=-NR*(NR-1)/(2.*NR-1)
0799                AP(NR1,NC)=CAD*AN1(NR)
0800                AP(NR1,NC1)=CAD*BN1(NR)
0801                AP(NR2,NC)=CAD*AN2(NR)
0802                AP(NR2,NC1)=CAD*BN2(NR)
0803                NR3=NR+L2P
0804                NR4=NC+L4+L8P+L8P+L8M
0805                NC2=NC+L2+L8P+L8P
0806                NC3=NR+L78
0807                AP(NR3,NC2)=-DEXP(UN1)
0808                AP(NR3,NC3)=-DEXP(-UN1)
0809                AP(NR4,NC2)=-DEXP(-UN2)
0810                AP(NR4,NC3)=-DEXP(UN2)
0811                CID=1./(2*NR-1.)
0812                AP(NR3,NC)=CID*AN1(NR)
0813                AP(NR3,NC1)=CID*BN1(NR)
0814                AP(NR4,NC)=CID*AN2(NR)
0815                AP(NR4,NC1)=CID*BN2(NR)
0816                NPP=NRP+1
0817                CODE=-1./(2*NR+3.)
0818                AP(NR3,NRP)=CODE*AN1(NPP)
0819                AP(NR3,NCP)=CODE*BN1(NPP)
0820                AP(NR4,NRP)=CODE*AN2(NPP)
0821          302   AP(NR4,NCP)=CODE*BN2(NPP)
0822                DO 303 NR=1,L8
0823                NR2=NR+L78
0824                NR1=NR+L34
0825                NC1=NR+L8
0826                NC2=NR+L4
0827                NC3=NR+L38
```

```
0828                NC4=NR+L2
0829                NC5=NR+L2+L8P
0830                NC4P=NC4+1
0831                NC5P=NC5+1
0832                CID=2.*(2*NR+1.)
0833                AP(NR1,NR)=CID
0834                AP(NR2,NC1)=-CID
0835                AP(NR1,NC2)=5.
0836                AP(NR2,NC3)=5.
0837                AP(NR1,NC4)=-1.
0838                AP(NR2,NC5)=-1.
0839                AP(NR1,NC4P)=2.
0840          303   AP(NR2,NC5P)=2.
0841                DO 304 NR=1,L8M
0842                NR1=NR+L34
0843                NR2=NR+L78
0844                NP=NR+1
0845                NR3=NP+L34
0846                NR4=NP+L78
0847                NC1=NR+L4
0848                NC2=NR+L38
0849                CN=NR
0850                AP(NR3,NC1)=-CN
0851                AP(NR4,NC2)=-CN
0852                NC3=NP+L4
0853                NC4=NP+L38
0854                AP(NR1,NC3)=NP+1.
0855                AP(NR2,NC4)=NP+1.
0856                NC5=L2+NR+2
0857                NC6=L2+L8P+2+NR
0858                AP(NR1,NC5)=-1.
0859                AP(NR2,NC6)=-1.
0860                NC7=L2+L8P+L8P+NR
0861                NC8=NC7+L8M
0862                AP(NR1,NC7)=(NR+2)*(NR+3.)
0863                AP(NR2,NC8)=(NR+2)*(NR+3.)
0864                AP(NR3,NC7)=-2.*NR*(NP+2)
0865                AP(NR4,NC8)=-2.*NR*(NP+2)
0866                NR5=NR+L8
0867                AP(NR3,NR)=-2.*NR
0868                AP(NR4,NR5)=+2.*NR
0869                NP1=NP+L8
0870                AP(NR1,NP)=-2.*(NR+2)
0871          304   AP(NR2,NP1)=+2.*(NR+2)
0872                DO 305 NR=3,L8
0873                NR1=NR+L34
```

```
0874                NM=NR-2
0875                NR2=NR+L78
0876                NC1=NM+L2+L8P+L8P
0877                NC2=NC1+L8M
0878                AP(NR1,NC1)=(NR-2.)*(NR-1)
0879           305  AP(NR2,NC2)=(NR-2.)*(NR-1)
0880                FACT1=+6.*PI*VIS*A1*2.*SQ2/3.*DSINH(U10)
0881                FACT2=+6.*PI*VIS*A2*2.*SQ2/3.*DSINH(U20)
0882                DO 306 NC=1,L8P
0883                NC1=NC+L2
0884                NC2=NC1+L8P
0885                AP(LP,NC1)=FACT1
0886           306  AP(LL,NC2)=FACT2
0887                BP(LP)=FPD1
0888                BP(LL)=FPD2
0889                AP(L8,L8P)=0
0890                AP(L8,L4P)=0
0891                AP(L4,L4P)=0
0892                AP(L4,L8P)=0
0893                AP(L58P,L8P)=0
0894                AP(L58P,L4P)=0
0895                AP(L34,L8P)=0
0896                AP(L34,L4P)=0
0897                L513=L4+L8P
0898                L713=L4+L8P+L8P
0899                AP(L513,L8P)=0
0900                AP(L513,L4P)=0
0901                AP(L713,L8P)=0
0902                AP(L713,L4P)=0
0903                ETS=.1E-16
0904                CALL DGELG(BP,AP,LL,1,ETS,IER)
0905                WRITE(3,55)
0906                WRITE(3,3)(BP(N),N=1,LL)
0907                WRITE(3,2)
0908                WRITE(3,25)
0909                WRITE(3,5)ETS,IER
0910                WRITE(3,2)
0911                WRITE(3,71)
0912                WRITE(3,1)FPD1,FPD2,FPD1P,FPD2P
0913                CHK1=C1*BP(97)+C5*BP(98)
0914                CHK2=C2*BP(97)+C6*BP(98)
0915                WRITE(3,72)
0916                WRITE(3,1)CHK1,CHK2
0917                DO 2000 N=1,L8
0918                UN1=(N+.5)*U10
0919                UN2=(N+.5)*U20
0920                NLA=N
0921                NLB=N+L8
0922                NLC=N+L4
0923                NLD=N+L38
```

```
0924                AB1(N)=(BP(NLA)*DEXP(UN1)+BP(NLB)*DEXP(-UN1))/DSINH(U10)
0925                AB2(N)=-(BP(NLA)*DEXP(-UN2)+BP(NLB)*DEXP(UN2))/DSINH(U20)
0926                ARAP(N)=BP(NLA)*DEXP(UN1)/DSINH(U10)
0927                ARBP(N)=BP(NLB)*DEXP(-UN1)/DSINH(U10)
0928                ARAM(N)=-BP(NLA)*DEXP(-UN2)/DSINH(U20)
0929                ARBM(N)=-BP(NLB)*DEXP(UN2)/DSINH(U20)
0930                CD1(N)=(BP(NLC)*DEXP(UN1)+BP(NLD)*DEXP(-UN1))
0931          2000  CD2(N)=+(BP(NLC)*DEXP(-UN2)+BP(NLD)*DEXP(UN2))
0932                DO 2001 N=1,L8P
0933                UN1=(N-.5)*U10
0934                UN2=(N-.5)*U20
0935                NLE=N+L2
0936                NLF=N+L2+L8P
0937                EF1(N)=(BP(NLE)*DEXP(UN1)+BP(NLF)*DEXP(-UN1))
0938          2001  EF2(N)=+(BP(NLE)*DEXP(-UN2)+BP(NLF)*DEXP(UN2))
0939                DO 2002 N=1,L8M
0940                UN1=(N+1.5)*U10
0941                UN2=(N+1.5)*U20
0942                NLG=N+L2+L8P+L8P
0943                NLH=N+L2+L8P+L8P+L8M
0944                GH1(N)=(BP(NLG)*DEXP(UN1)+BP(NLH)*DEXP(-UN1))
0945          2002  GH2(N)=+(BP(NLG)*DEXP(-UN2)+BP(NLH)*DEXP(UN2))
0946                DO 2003 N=1,L8
0947                AB1(L8P)=0
0948                AB2(L8P)=0
0949                K=N+1
0950                M=N-1
0951                IF (M)2004,2004,2005
0952          2004  M=N
0953          2005  ARB1=-2*(N+2)/(2*N+3.)*AB1(K)
0954                BRB1=-2*(N+2)/(2*N+3.)*AB2(K)
0955                ARB2=2*DCOSH(U10)*AB1(N)
0956                BRB2=2*DCOSH(U20)*AB2(N)
0957                ARB3=-(N-1)/(2*N-1.)*AB1(M)*2.
0958                BRB3=-(N-1)/(2*N-1.)*AB2(M)*2.
0959                CND11=CD1(N)+ARB1+ARB2+ARB3
0960                CND12=CD2(N)+BRB1+BRB2+BRB3
0961                WRITE(3,78) N
0962                WRITE(3,82)
0963          2003  WRITE(3,1)CND11,CND12
0964                DO 2006 N=1,L8P
0965                UN1=(N-.5)*U10
0966                UN2=(N-.5)*U20
0967                K=N+1
0968                M=N-1
0969                MM=M-1
```

```
0970                AB1(L8P)=0
0971                AB2(L8P)=0
0972                ARB1=-2*BP(LP)*SQ2*DEXP(-UN1)
0973                BRB1=-2*BP(LL)*SQ2*DEXP(-UN2)
0974                ARB2=-(M+1)*(M+2)/(2*M+3.)*AB1(N)
0975                BRB2=-(M+1)*(M+2)/(2*M+3.)*AB2(N)
0976                IF (MM)2007,2007,2008
0977          2007  MM=N
0978          2008  ARB3=M*(M-1)/(2*M-1.)*AB1(MM)
0979                BRB3=M*(M-1)/(2*M-1.)*AB2(MM)
0980                CND21=EF1(N)+ARB1+ARB2+ARB3
0981                CND22=EF2(N)+BRB1+BRB2+BRB3
0982                WRITE(3,78) N
0983                WRITE(3,83)
0984          2006  WRITE(3,1)CND21,CND22
0985                DO 2009 N=1,L8M
0986                K=N+1
0987                KK=N+2
0988                AB1(L8P)=0
0989                AB2(L8P)=0
0990                ARAP(L8P)=0.
0991                ARAM(L8P)=0.
0992                 ARBM(L8P)=0.
0993                ARBP(L8P)=0.
0994                ARB1=GH1(N)
0995                BRB1=GH2(N)
0996                CID=1./(2.*K-1.)
0997                CODE=1./(2.*K+3.)
0998                ARB2A=-CID*ARAP(N)
0999                BRB2A=-CID*ARAM(N)
1000                ARB2B=-CID*ARBP(N)
1001                BRB2B=-CID*ARBM(N)
1002                ARB2=ARB2A+ARB2B
1003                BRB2=BRB2A+BRB2B
1004                ARB3A=CODE*ARAP(KK)
1005                BRB3A=CODE*ARAM(KK)
1006                ARB3B=CODE*ARBP(KK)
1007                BRB3B=CODE*ARBM(KK)
1008                ARB3=ARB3A+ARB3B
1009                BRB3=BRB3A+BRB3B
1010                CND31=ARB1+ARB2+ARB3
1011                CND32=BRB1+BRB2+BRB3
1012                WRITE(3,78) N
1013                WRITE(3,84)
1014          2009  WRITE(3,1)CND31,CND32
```

```
1015              NUMB=L2P+L8P
1016              CND41=BP(L2P)
1017              CND42=-BP(NUMB)
1018              CND51=0.
1019              CND52=0.
1020              WRITE(3,85)
1021              DO 2010 N=1,L8
1022              M=N-1
1023              NLA=N
1024              NLB=N+L8
1025              NLE=N+L2
1026              NLF=N+L2+L8P
1027              NLEP=NLE+1
1028              NLFP=NLF+1
1029              CND41=CND41+2.*N*(N+1.)*BP(NLA)+(2.*N+1.)*BP(NLEP)
1030              CND42=CND42+2.*N*(N+1.)*BP(NLB)-(2.*N+1.)*BP(NLFP)
1031         2010 WRITE(3,1)CND41,CND42
1032              DO 2011 N=1,L8P
1033              NLE=N+L2
1034              NLF=N+L2+L8P
1035              CND51=CND51+BP(NLE)
1036         2011 CND52=CND52+BP(NLF)
1037              CND52=FPD2-6.*PI*VIS*A2*2.*SQ2/3.*DSINH(U20)*CND52
1038              CND51=FPD1-6.*PI*VIS*A1*2.*SQ2/3.*DSINH(U10)*CND51
1039              WRITE(3,86)
1040              WRITE(3,1)CND51,CND52
1041              V1PD=BP(LP)
1042              V2PD=BP(LL)
1043              V1X=V1PL*DSIN(ALF)-V1PD*DCOS(ALF)
1044              V1Z=V1PL*DCOS(ALF)+V1PD*DSIN(ALF)
1045              V2X=V2PL*DSIN(ALF)-V2PD*DCOS(ALF)
1046              V2Z=V2PL*DCOS(ALF)+V2PD*DSIN(ALF)
1047              VE1X(JE)=V1X
1048              VE2X(JE)=V2X
1049              VE1Z(JE)=V1Z
1050              VE2Z(JE)=V2Z
1051              WRITE(3,96)
1052              WRITE(3,1)V1X,V2X,V1Z,V2Z
1053              W1X(IND)=V1X
1054              IF (IND-2)602,603,603
1055          603 X1P=(W1X(1)+W1X(2))*DT/4.+W1X(1)*DT/2.+X1W(1)
1056              IF (DABS(X1P-X1W(2))-ERR1)604,604,605
1057          604 INDP=INDP+1
1058              IF (INDP-3)602,607,607
1059          607 IF (DABS((W1X(1)+W1X(3))/2.-W1X(2))-ERR2)608,608,602
1060          608 DT=2.*DT
1061              WRITE(3,98)
```

```
1062                IND=0
1063                GO TO 602
1064          605   DT=DT/2.
1065                WRITE(3,97)
1066                INDP=1
1067                X1=X1-V1XN*DT
1068                X2=X2-V2XN*DT
1069                Z1=Z1-V1ZN*DT
1070                Z2=Z2-V2ZN*DT
1071                GO TO 606
1072          602   CONTINUE
1073                X1=X1+V1X*DT
1074                X2=X2+V2X*DT
1075                Z1=Z1+V1Z*DT
1076                Z2=Z2+V2Z*DT
1077                DX=X1-X2
1078                DZ=Z1-Z2
1079                CHGX(JE)=DX
1080                CHGZ(JE)=DZ
1081                JE=JE+1
1082                IF (DZ) 833,834,833
1083          834   ALF=PI/2
1084                GO TO 836
1085          833   ALF=DATAN(DX/DZ)
1086          836   ARUG=DZ*DZ+DX*DX
1087                DA=DSQRT(ARUG)
1088                WRITE(3,63)
1089                WRITE(3,65)
1090                TT=TT+DT
1091                WRITE(3,1)DA,ALF,TT
1092                WRITE(3,95)
1093                WRITE(3,1)X1,X2,Z1,Z2
1094                WRITE(3,40)
1095                IF (DA-.0120)850,838,838
1096          850   GO TO 800
1097          838   CONTINUE
1098                JE=JE-1
1099                WRITE(3,99)
1100                WRITE(3,3)(DIST(N),ANGL(N),VE1X(N),VE1Z(N),VE2X(N),VE2Z(N),N=1,JE)
1101                WRITE(3,75)
1102                WRITE(3,100)(DIST(N),FOR1(N),FOR2(N),N=1,JE)
1103                WRITE(3,1)(CHGX(N),CHGZ(N),N=1,JE)
1104                RETURN
1105                END
```